1970

Spread of Plasticity from the Tip of a Penny-Shaped Crack

Zong Shyong Luo

SPREAD OF PLASTICITY FROM THE TIP OF A PENNY-SHAPED CRACK

BY

ZONG SHYONG LUO

A thesis submitted
in partial fulfillment of the requirements for the
degree Master of Science, Major in
Mechanical Engineering, South
Dakota State University

1970

SPREAD OF PLASTICITY FROM THE TIP

OF A PENNY-SHAPED CRACK

This thesis is approved as a creditable and independent investigation by a candidate for the degree, Master of Science, and is acceptable as meeting the thesis requirements for this degree, but without implying that the conclusions reached by the candidate are necessarily the conclusions of the major department.

Thesis Adviser Date

Head, Mechanical Engineering Department Date

ACKNOWLEDGMENTS

Having finished my Master's program, I would like to express my appreciation and gratitude to all of my teachers whose effort is directly or indirectly reflected in this program. I am specially indebted to Dr. Milosz P. Wnuk for his many valuable comments and his helpful discussions. Courses taught by Professors Walder, Juricic and Lumsdaine greatly enhanced my background needed to finish this thesis.

My thanks are also due to Professor John F. Sandfort, Head of Mechanical Engineering Department, for suggesting this interesting field and for his constant encouragement.

ZSL

TABLE OF CONTENTS

LIST OF SYMBOLS

Symbol	Meaning
r, θ, z	Cylindrical coordinates
$^{o}\epsilon_r, {}^{o}\epsilon_\theta, {}^{o}\epsilon_z$	Purely elastic normal strains
$^{o}\sigma_r, {}^{o}\sigma_\theta, {}^{o}\sigma_z$	Purely elastic normal stresses
$^{o}\gamma_{r\theta}, {}^{o}\gamma_{\theta z}, {}^{o}\gamma_{zr}$	Purely elastic shear stresses
$^{o}\tau_{r\theta}, {}^{o}\tau_{\theta z}, {}^{o}\tau_{zr}$	Pure elastic shear strains
E, G	Young's modulus and shear modulus
ν	Poisson's ratio
u_r, u_θ, u_z	Displacement in r, θ, and z directions, respectively
$^{e}\epsilon_r, {}^{e}\epsilon_\theta, {}^{e}\epsilon_z$	Elastic normal strains
$^{e}\sigma_r, {}^{e}\sigma_\theta, {}^{e}\sigma_z$	Elastic normal stresses
$^{e}\gamma_{r\theta}, {}^{e}\gamma_{\theta z}, {}^{e}\gamma_{zr}$	Elastic normal strains
$^{e}\tau_{r\theta}, {}^{e}\tau_{\theta z}, {}^{e}\tau_{zr}$	Elastic shear stresses
$^{p}\gamma_{r\theta}, {}^{p}\gamma_{\theta z}, {}^{p}\gamma_{zr}$	Plastic shear strains
$^{p}\tau_{r\theta}, {}^{p}\tau_{\theta z}, {}^{p}\tau_{zr}$	Plastic shear stresses
$^{p}\sigma_r, {}^{p}\sigma_\theta, {}^{p}\sigma_z$	Plastic normal stresses
$^{p}\epsilon_r, {}^{p}\epsilon_\theta, {}^{p}\epsilon_z$	Plastic normal strains
σ_i	Stress intensity
ϵ_i	Strain intensity
Y	Yield stress at uniaxial tension
^{e}u	Elastic strain energy density
^{p}u	Plastic strain energy density

Symbol	Meaning
U	Total strain energy
W	Work of external forces
Π	Potential energy of the system
L	Half of major axis of the crack
δ_1	Distance measured from the crack tip
λ	Dimensionless load
ψ	Angle measured at the crack tip
ϕ	Generalized modulus of plastic deformation
σ_1	Maximum principal stress
σ_m	Medium stress
P_{crit}	Critical stress
SE	Surface energy
γ	Specific surface energy
S	Dimensionless crack length

CHAPTER I

INTRODUCTION

1.1. Historical Background

With the increasing attention to failure problems over the last half century went a growing interest in the fracture process in materials. Many previous investigators have studied the elastic distributions around the cracks basing on the idea of Inglis [1]* who in 1913 was the first to study an internal crack by use of the elliptical bounding surfaces. Probably the most important concept put forth in this field was Griffith's hypothesis [2] of a brittle fracture which was published in 1921. Employing the idea of Inglis and the principle of conservation of energy, Griffith derived a theoretical formula for the critical stress at the crack tip and a criterion for crack instability.

A simplification of the energy method as initiated by Griffith has been given by Irwin [3] who analyzed the energy exchange in the immediate vicinity of the crack tip. Later Sander [4] expressed the Griffith-Irwin criterion for crack extension in the form of a contour integral. Meanwhile substantial work was done by Sneddon [5] and by Sack [6] in Great Britain. They have derived expressions for the critical stress around a penny-shaped crack in an elastic

---

*Bracketed numbers refer to the references.

solid. In the United States, Westergaard [12] initially introduced the complex variable technique into three-dimensional problems, and Williams [14] gave a supplement on the problem of cracks by working out relations for antisymmetric cases.

The energy point of view of fracture phenomena has been widely and successfully developed by contemporary scientists, such as Orowan [7], Mott [8], Berry [9], Goodier and Field [10], and Dugdale [11], etc.

It is of interest to note that there exist different points of view concerning the magnitudes of stresses around the crack tip. However, all investigators are unanimous in the assertion that near the origin of the crack there is a very high stress concentration. It is quite obvious that these ultimate stresses may lead not only to the development of the crack, but also to changes in the material itself. Therefore, the elastic-plastic energy criterion was developed. The work done by Olesiak and Wnuk [17], and by Wnuk [15, 16] can be considered the major step into the extension of energy consideration to elastic-plastic materials. In those works, various types of fractures were discussed on the basis of energy consideration, and a new model of a crack with associated plastic zones extending from the tip of the crack was developed. An equation for critical stress at the crack tip was also developed. The difference between elasticity and plasticity in fracture mechanics has not been yet adequately clarified.

To the author's knowledge, we are now in a period when higher-strength materials, new design ideas, and pressures from the competition demand an ability to plan for fracture safety in situations where past experience is very limited. If fracture mechanics is to be used in the design of structures, a better understanding of the mechanism of crack extension is indispensable. In this thesis, a new idea about the elastic-plastic stress distribution at the crack tip is introduced. A modification of the elastic-plastic boundary due to the crack-tip-shifting phenomenan is investigated. Also, a set of equations governing the elastic-plastic stress and energy distribution close to the fracture front are derived in the thesis. Finally, a modified fracture criterion is presented to make the thesis complete.

1.2. Thesis Outline

In the study of fracture mechanics in solids, the major interest centers around the crack tip zone. A penny-shaped crack having the diameter 2L is introduced for investigation. As mentioned, there will exist a plastic zone due to the high stress concentration and it is located at the crack tip. A plausible explanation for such plastic behavior develops from continuum mechanics. It has been shown [18] that the density, and consequently the volume, does not change even for very large plastic deformations. Thus, in the plastic range, a material can be considered as incompressible, (see Appendix I).

In Chapter II, the elastic and plastic stress components are postulated within the accuracy of certain unknown parameters. The generalized Hooke's law is employed for the elastic region, while the plastic stress and strain components are obtained through the application of the Huber-Mises-Hencky plasticity condition and the Hencky-Ilyushin constitutive equations. The stress analysis results in equations (2.3.1) and (2.3.7a) indicate there is an inverse square-root stress singularity at the "shifted" crack leading edge. This stress singularity is the driving force for the crack tip to propagate. The common elastic-plastic stress components along the boundary have been derived in equations (2.5.13-18). The deviatoric stress components which govern the yielding condition are given by equations (2.4.1) and (2.4.2). All these distributions are shown in plots.

With increasing applied load, for instance for tension perpendicular to the crack surface, a small plastic zone develops at the leading edge of the crack. Within this zone stresses are required to obey the plasticity equations. Some crack tip investigations indicated the interesting fact that the apparent tip of the crack is shifted with respect to the true crack front. The shifting distance under the antiplane shear condition was found by Rice [19]. Interestingly it was equal to the half of the plastic zone dimension.

Our own investigation of the crack tip shifting effect for the tensile fracture mode of equation (3.3.4) agrees well with Rice's observation at least for one particular case of $\beta = \frac{1}{2}$.

Equation (3.3.4) is believed to be the unified equation of the crack tip shifting distance. It is valid for different strengths of singularity β.

In Chapter IV, after evaluating the energy densities, with the application of minimum potential energy principle, the generalized elastic-plastic modification factor "A" which was introduced in Chapter II, can be determined. The final result in equation (4.3.10) shows that the factor "A" is a function of Poisson's ratio as well as the dimensionless load λ. Also, the effect of the type of stress singularity is discussed.

The critical stress is evaluated in Chapter V by using the energy components from Chapter IV and the principle of energy balance. The result presented by equation (5.3.10) is found to deviate from the one obtained by Sack and Sneddon [6,5] for a purely elastic solid. The discrepancy is particularly pronounced for a crack length of order K_{IC}^2 / Y^2 or less, where K_{IC} denotes the Irwin K-factor. Of course our result is only an approximation but it indicates a trend. For a crack length equal to the characteristic length $\frac{1}{2\pi} K_{IC}^2 / Y^2$, the critical stress for the elastic-plastic solid becomes a constant, while for a purely elastic solid the critical stress approaches infinity. This is shown in Figure 22.

In the last part of this thesis, Chapter VI, the important summary of results is presented along with an engineering discussion of the applicability of the thesis.

The supplementary analyses of the coefficient of lateral plastic deformation and reduced crack tip shifting distance are included in Appendix I and II.

CHAPTER II

ELASTIC AND PLASTIC ANALYSES AROUND THE PENNY-SHAPED CRACK

The stress and strain components of the elastic and plastic regions around the crack tip will be derived for a particular geometry. The geometry chosen here is that of an infinitely large body, as shown in Figure 1, having a central circular crack of diameter 2L. The elastic body is loaded with stress P_o in the Z-direction at an infinite edge. A cylindrical coordinate system (r, z, θ) is used. The initial crack will remain stationary or tend to extend. The experimental evidence indicates that there is a plastic region developed in the very vicinity of the crack tip. Our aim in this paper is to determine theoretically the shape of this region and the amount of energy dissipated therein. After a kinematically admissible strain field is chosen, the remaining free parameters will be determined by use of the variational extreme principle. The critical stress which precipitates the catastrophic fracture, will be derived from an energy balance criterion, which is similar in form to the Griffith equation except for the new correction term. The term results from the plastic energy dissipation expended on the irreversible deformation in the vicinity of the crack front. As this approach is based upon the dominant singularity only, it should be noted, that the validity of the correction term appearing in the fracture criterion is restricted to small values of load to yield stress ratio.

It will be shown that when the ratio of applied load to the yield stress tends to zero our result reduces to the Griffith classical formulas.

2.1. Postulation of Strain Components in Elastic Region

Sneddon's solution for purely elastic stress field is used in postulating new elastic and plastic strains in the front of the crack tip. The elastic stress distribution found by Sneddon [5] in the immediate vicinity of the fracture front is

$$
\left.
\begin{aligned}
{}^{o}\sigma_r &= \frac{2P_o}{\pi}\left(\frac{1}{2\delta}\right)^{\frac{1}{2}}\left(\frac{3}{4}\cos\frac{\psi}{2} + \frac{1}{4}\cos\frac{5\psi}{2}\right) + O(\delta^{\frac{1}{2}}) \\
{}^{o}\sigma_\theta &= \frac{2P_o}{\pi}\left(\frac{1}{2\delta}\right)^{\frac{1}{2}}\left(2\nu\cos\frac{\psi}{2}\right) + O(\delta^{\frac{1}{2}}) \\
{}^{o}\sigma_z &= \frac{2P_o}{\pi}\left(\frac{1}{2\delta}\right)^{\frac{1}{2}}\left(\frac{5}{4}\cos\frac{\psi}{2} - \frac{1}{4}\cos\frac{5\psi}{2}\right) + O(\delta^{\frac{1}{2}}) \\
{}^{o}\tau_{rz} &= \frac{2P_o}{\pi}\left(\frac{1}{2\delta}\right)^{\frac{1}{2}}\left(\frac{1}{2}\sin\psi\cos\frac{3\psi}{2}\right) + O(\delta^{\frac{1}{2}}) \\
{}^{o}\tau_{r\theta} &= {}^{o}\tau_{\theta z} = 0
\end{aligned}
\right\} \quad (2.1.1)
$$

where P_o denotes the stress applied perpendicular to the crack surface in the Z-direction, δ is the ratio of the coordinate δ_1 to the half crack length L (see Figure 1). The term $O(\delta^{\frac{1}{2}})$ vanishes for $\delta \to o$ and is assumed to be negligibly small in the entire considered region, i.e. close to the crack front.

Knowing the stress components, we may apply the generalized Hooke's law to find the elastic strain distribution

$$
\left.
\begin{aligned}
{}^{o}\epsilon_r &= \frac{1}{E}\left[{}^{o}\sigma_r - \nu({}^{o}\sigma_\theta + {}^{o}\sigma_z)\right] \\
{}^{o}\epsilon_\theta &= \frac{1}{E}\left[{}^{o}\sigma_\theta - \nu({}^{o}\sigma_z + {}^{o}\sigma_r)\right] \\
{}^{o}\epsilon_z &= \frac{1}{E}\left[{}^{o}\sigma_z - \nu({}^{o}\sigma_r + {}^{o}\sigma_\theta)\right] \\
{}^{o}\gamma_{r\theta} &= \frac{2(1+\nu)}{E}\,{}^{o}\tau_{r\theta} \\
{}^{o}\gamma_{\theta z} &= \frac{2(1+\nu)}{E}\,{}^{o}\tau_{\theta z} \\
{}^{o}\gamma_{zr} &= \frac{2(1+\nu)}{E}\,{}^{o}\tau_{zr}
\end{aligned}
\right\} \quad (2.1.2)
$$

After some manipulation, the corresponding elastic strains are found as

$$
\left.
\begin{aligned}
{}^{o}\epsilon_r &= \frac{P_o(1+\nu)}{2\pi E}\left(\frac{1}{2\delta}\right)^{\frac{1}{2}}\left(4h\cos\frac{\psi}{2} - 2\sin\frac{3\psi}{2}\sin\psi\right) \\
{}^{o}\epsilon_\theta &= \frac{P_o(1+\nu)}{2\pi E}\left(\frac{1}{2\delta}\right)^{\frac{1}{2}}\cdot 0 = 0 \\
{}^{o}\epsilon_z &= \frac{P_o(1+\nu)}{2\pi E}\left(\frac{1}{2\delta}\right)^{\frac{1}{2}}\left(4h\cos\frac{\psi}{2} + 2\sin\frac{3\psi}{2}\sin\psi\right) \\
{}^{o}\gamma_{zr} &= \frac{P_o(1+\nu)}{2\pi E}\left(\frac{1}{2\delta}\right)^{\frac{1}{2}}\left(4\sin\psi\cos\frac{3\psi}{2}\right) \\
{}^{o}\gamma_{r\theta} &= {}^{o}\gamma_{\theta z} = 0
\end{aligned}
\right\} \quad (2.1.3)
$$

where

$$h = 1 - 2\nu \tag{2.1.3a}$$

or re-writing equation (2.1.3) in a shortened form, we have

$$\left.\begin{aligned} {}^{o}\epsilon_r &= \frac{K}{\sqrt{2\delta}} R(\psi) \\ {}^{o}\epsilon_\theta &= \frac{K}{\sqrt{2\delta}} \theta(\psi) \\ {}^{o}\epsilon_z &= \frac{K}{\sqrt{2\delta}} Z(\psi) \\ {}^{o}\gamma_{zr} &= \frac{K}{\sqrt{2\delta}} ZR(\psi) \end{aligned}\right\} \tag{2.1.4}$$

where, by comparing with equation (2.1.3) and equations (2.1.4), the values of K-factor and the angular functions are

$$\left.\begin{aligned} K &= \frac{P_o(1+\nu)}{2E} \\ R(\psi) &= 4h \cos\frac{\psi}{2} - 2 \sin\frac{3\psi}{2} \sin\psi \\ \theta(\psi) &= 0 \\ Z(\psi) &= 4h \cos\frac{\psi}{2} + 2 \sin\frac{3\psi}{2} \sin\psi \\ ZR(\psi) &= 4 \sin\frac{3\psi}{2} \sin\psi \end{aligned}\right\} \tag{2.1.5}$$

As we have mentioned, the classical stress and strain analyses by Sneddon, true for a purely elastic solid, are not descriptive to the real material behavior. Therefore we shall investigate certain stress and strain fields which will better account for both the elastic and plastic behavior of the material due to the high stress concentration at the crack tip.

Here, let us postulate the strains outside the plastic zone but still close to the crack tip; only the dominant singularity term is taken into account. Using the tensorial notation based on the Sneddon's strain field ${}^{o}\epsilon_{ij}$, we have

$$ {}^{e}\epsilon_{ij} = {}^{e}A \left[\frac{2\delta}{2(\delta - \delta_o)}\right]^{\frac{1}{2}} {}^{o}\epsilon_{ij} \qquad (2.1.6) $$

We assume that although the angular distributions R, θ, Z and ZR do not change, they are shifted away from the crack tip by a certain distance δ_o. The amplitude ${}^{e}A$ will be left as a free parameter subject to determination. The elastic modification factor and crack tip shifting distance will be investigated in the following chapters.

The tensorial relationship in (2.1.6) is expanded in the following way

$$ {}^{e}\epsilon_{r} = \frac{{}^{e}AK}{\left[2(\delta - \delta_o)\right]^{\frac{1}{2}}} R(\psi) $$

$$
\left.
\begin{aligned}
{}^{e}\epsilon_{\theta} &= \frac{{}^{e}A_{K}}{\left[2(\delta - \delta_{o})\right]^{\frac{1}{2}}}\,\Theta(\psi) \\
{}^{e}\epsilon_{z} &= \frac{{}^{e}A_{K}}{\left[2(\delta - \delta_{o})\right]^{\frac{1}{2}}}\,Z(\psi) \\
{}^{e}\gamma_{zr} &= \frac{{}^{e}A_{K}}{\left[2(\delta - \delta_{o})\right]^{\frac{1}{2}}}\,ZR(\psi) \\
{}^{e}\gamma_{r\theta} &= {}^{e}\gamma_{\theta z} = 0
\end{aligned}
\right\} \qquad (2.1.7)
$$

2.2. Postulation of Strain Components in the Plastic Region

A similar approach can be applied in dealing with the strain components in the plastic region.

Invoking the experimental evidence gathered by Gerberich and Swedlow [20], we may postulate plastic strains in the following way

$$
{}^{p}\epsilon_{ij} = \frac{{}^{p}A\sqrt{2\delta}}{\delta^{\beta}}\,{}^{o}\epsilon_{ij} \qquad (2.2.1)
$$

The strength of singularity β in the above equation may vary between $\beta = \frac{1}{2}$ for a limiting case of a purely brittle solid and $\beta = 1$ for a perfectly elastic-plastic solid. The intermediate values of β correspond to a certain amount of strain-hardening, $\frac{1}{2} \leq \beta \leq 1$, c.f. Hutchinson [21].

In expanded forms equation (2.2.1) reads

$$
\left.
\begin{aligned}
{}^{p}\epsilon_{r} &= \frac{{}^{p}A_{K}}{\delta^{\beta}}\,R(\psi) \\
{}^{p}\epsilon_{\theta} &= \frac{{}^{p}A_{K}}{\delta^{\beta}}\,\Theta(\psi)
\end{aligned}
\right\}
$$

$$
\left.
\begin{aligned}
{}^{p}\epsilon_z &= \frac{p_{AK}}{\delta^{\beta}}\, Z(\psi) \\
{}^{p}\gamma_{zr} &= \frac{p_{AK}}{\delta^{\beta}}\, ZR(\psi) \\
{}^{p}\gamma_{r\theta} &= {}^{p}\gamma_{\theta z} = 0
\end{aligned}
\right\} \qquad (2.2.2)
$$

For convenience in further derivations, let us assume the elastic and plastic modification factors have the same value, therefore

$$ {}^{e}A = {}^{p}A = A \qquad (2.2.3) $$

This constant A will be called the generalized elastic-plastic modification factor in the following chapters.

2.3. Derivation of the Stress Components in Elastic and Plastic Regions

By applying the generalized Hooke's law and substituting the functions R, θ, Z and ZR, the stresses for the elastic region take the form

$$
\left.
\begin{aligned}
{}^{e}\sigma_r &= \frac{2YA\lambda}{\pi}\left[2(\delta-\delta_o)\right]^{-\frac{1}{2}}\left(\frac{3}{4}\cos\frac{\psi}{2}+\frac{1}{4}\cos\frac{5\psi}{2}\right) \\
{}^{e}\sigma_\theta &= \frac{2YA\lambda}{\pi}\left[2(\delta-\delta_o)\right]^{-\frac{1}{2}}\left(2\nu\cos\frac{\psi}{2}\right) \\
{}^{e}\sigma_z &= \frac{2YA\lambda}{\pi}\left[2(\delta-\delta_o)\right]^{-\frac{1}{2}}\left(\frac{5}{4}\cos\frac{\psi}{2}-\frac{1}{4}\cos\frac{5\psi}{2}\right) \\
{}^{e}\tau_{zr} &= \frac{2YA\lambda}{\pi}\left[2(\delta-\delta_o)\right]^{-\frac{1}{2}}\left(\frac{1}{2}\sin\psi\cos\frac{3\psi}{2}\right) \\
{}^{e}\tau_{r\theta} &= {}^{e}\tau_{\theta z} = 0
\end{aligned}
\right\} \qquad (2.3.1)
$$

Here Y is the yield stress of the material at uniaxial tension. The dimensionless load is defined as

$$\lambda = \frac{P_o}{Y} \tag{2.3.2}$$

Again, note that the shift distance $\mathcal{E}_o$, the singularity strength β and generalized elastic-plastic modification factor A are yet unknown and they are subject to determination in later chapters.

In deriving the plastic stresses, since Hooke's law is no longer applicable in plastic region, we have to make use of some non-linear theorems of the theory of plasticity. If we choose to apply the Hencky-Ilyushin theory, then the plastic stress-strain relations are given as follows

$$\left.\begin{aligned} {}^{p}\epsilon_r - {}^{p}\epsilon_\theta &= \phi\,({}^{p}\sigma_r - {}^{p}\sigma_\theta) \\ {}^{p}\epsilon_\theta - {}^{p}\epsilon_z &= \phi\,({}^{p}\sigma_\theta - {}^{p}\sigma_z) \\ {}^{p}\epsilon_z - {}^{p}\epsilon_r &= \phi\,({}^{p}\sigma_z - {}^{p}\sigma_r) \\ \tfrac{1}{2}{}^{p}\gamma_{zr} &= \phi\,{}^{p}\tau_{zr} \end{aligned}\right\} \tag{2.3.3}$$

where $\phi = \phi\,(r,\theta,z)$ is a function named the generalized modulus of plastic deformation [18].

In the elastic region and at the boundary between both regions the value of ϕ is a constant, i.e.

$$\phi = \frac{1}{2G} \tag{2.3.4}$$

In order to solve equations (2.3.3) for plastic stresses, we will have to introduce more relationships. First of all we employ the criterion given by Huber-Mises-Hencky according to which "yielding

takes place whenever the stress intensity ${}^{p}\sigma_i$ reaches the yield stress Y of the material at simple tension", or mathematically,

$$ {}^{p}\sigma_i = \frac{1}{\sqrt{2}} \Big[({}^{p}\sigma_r - {}^{p}\sigma_\theta)^2 + ({}^{p}\sigma_\theta - {}^{p}\sigma_z)^2 + ({}^{p}\sigma_z - {}^{p}\sigma_r)^2 $$

$$ + 6\,({}^{p}\tau_{r\theta}{}^2 + {}^{p}\tau_{\theta z}{}^2 + {}^{p}\tau_{zr}{}^2) \Big]^{\frac{1}{2}} = Y \qquad (2.3.5) $$

Second, the dilatational stress-strain relation in the theory of elasticity can be applied equally well in plasticity for small strains, i.e.

$$ {}^{p}\sigma_r + {}^{p}\sigma_\theta + {}^{p}\sigma_z = \frac{AE}{1-2\nu} ({}^{o}\epsilon_r + {}^{o}\epsilon_\theta + {}^{o}\epsilon_z) \qquad (2.3.6) $$

With equations (2.2.2) and the six equations from (2.3.3), (2.3.5) and (2.3.6) in which five of them are independent, we can solve for the plastic stress components.

After some mathematical manipulation, we obtain the plastic stresses as follows

$$ {}^{p}\sigma_r = \frac{1}{3} \Big[\frac{P_o A}{\delta^\beta \pi} (1+\nu) \left(4 \cos \frac{\psi}{2}\right) + \frac{Y}{m(\psi)} \left(-3 \sin \psi \sin \frac{3\psi}{2} \right.$$

$$ \left. + 2h \cos \frac{\psi}{2}\right) \Big] $$

$$ {}^{p}\sigma_\theta = \frac{1}{3} \Big[\frac{P_o A}{\delta^\beta \pi} (1+\nu) \left(4 \cos \frac{\psi}{2}\right) - \frac{Y}{m(\psi)} \left(4h \cos \frac{\psi}{2}\right) \Big] $$

$$
\begin{aligned}
{}^{p}\sigma_z &= \frac{1}{3}\left[\frac{P_o A}{\delta^{\beta}\pi}(1+\nu)\left(4\cos\frac{\psi}{2}\right) + \frac{Y}{m(\psi)}\left(3\sin\psi\,\sin\frac{3\psi}{2}\right.\right. \\
&\quad \left.\left. + 2h\cos\frac{\psi}{2}\right)\right] \qquad (2.3.7)\\
{}^{p}\tau_{zr} &= \frac{Y}{m(\psi)}\sin\psi\,\cos\frac{3\psi}{2} \\
{}^{p}\tau_{r\theta} &= {}^{p}\tau_{\theta z} = 0
\end{aligned}
$$

where the notations are

$$
\left.
\begin{aligned}
m(\psi) &= \left(3\sin^2\psi + 4h^2\cos^2\frac{\psi}{2}\right)^{\frac{1}{2}} \\
h &= 1-2\nu
\end{aligned}
\right\} \qquad (2.3.7b)
$$

Equations (2.3.7) are the general forms for plastic stresses. For the strength singularity β equal to $\frac{1}{2}$, the plastic stresses in the plastic region close to the boundary become

$$
\left.
\begin{aligned}
{}^{p}\sigma_r &= \frac{1}{3}\left[\frac{P_o A}{\sqrt{\delta}\pi}(1+\nu)\left(4\cos\frac{\psi}{2}\right) + \frac{Y}{m(\psi)}\cdot\right. \\
&\quad \left.(-3\sin\psi\,\sin\frac{3\psi}{2} + 2h\cos\frac{\psi}{2})\right] \\
{}^{p}\sigma_\theta &= \frac{1}{3}\left[\frac{P_o A}{\sqrt{\delta}\pi}(1+\nu)\left(4\cos\frac{\psi}{2}\right) - \frac{Y}{m(\psi)}\cdot\right. \\
&\quad \left.(4h\cos\frac{\psi}{2})\right] \\
{}^{p}\sigma_z &= \frac{1}{3}\left[\frac{P_o A}{\sqrt{\delta}\pi}(1+\nu)\left(4\cos\frac{\psi}{2}\right) + \frac{Y}{m(\psi)}\cdot\right. \\
&\quad \left.(3\sin\psi\,\sin\frac{3\psi}{2} + 2h\cos\frac{\psi}{2})\right] \\
{}^{p}\tau_{zr} &= \frac{Y}{m(\psi)}\sin\psi\,\cos\frac{3\psi}{2} \\
{}^{p}\tau_{r\theta} &= {}^{p}\tau_{\theta z} = 0
\end{aligned}
\right\} \qquad (2.3.7a)
$$

In making a comparison among the results of equations (2.1.1), (2.3.1) and (2.3.7a), the stress component ${}^{p}\sigma_z$ has been taken as an example and plotted in Figure 2.

2.4. Deviatoric Stress Components

Equations (2.3.7a) determine the plastic stresses close or along the boundary. In this section we will work out the deviatoric stress components which in fact govern the yielding process.* Using (2.3.7a) we can write the components of the plastic stress deviator as follows

$$
\left.
\begin{aligned}
{}^{p}\sigma_r - {}^{p}\sigma_\theta &= \frac{Y}{3\,m(\psi)}\left(-3\sin\psi\,\sin\frac{3\psi}{2} + 6h\cos\frac{\psi}{2}\right)\\
{}^{p}\sigma_\theta - {}^{p}\sigma_z &= \frac{Y}{3\,m(\psi)}\left(-3\sin\psi\,\sin\frac{3\psi}{2} - 6h\cos\frac{\psi}{2}\right)\\
{}^{p}\sigma_z - {}^{p}\sigma_r &= \frac{Y}{3\,m(\psi)}\left(6\sin\psi\,\sin\frac{3\psi}{2}\right)\\
{}^{p}\tau_{zr} &= \frac{Y}{3\,m(\psi)}\left(3\sin\psi\,\sin\frac{3\psi}{2}\right)\\
{}^{p}\tau_{r\theta} &= {}^{p}\tau_{\theta z} = 0
\end{aligned}
\right\} \qquad (2.4.1)
$$

The graphical distributions of these deviatoric stresses are shown in Figure 3, 4, 5 and 6. It is seen that the singular terms do cancel out and the deviatoric stress is therefore constant for a fixed value of ψ.

*P. W. Bridgeman [25] has demonstrated that the hydrostatic part of the stress tensor even at very high normal pressures has little influence on the yielding process.

Similarly, the elastic deviatoric stress components can be derived from equations (2.3.1). Here the singular terms do not cancel and we recover the classical singularity of the inverse square-root type. The difference between these expressions and Sneddon's solution is in the shifting distance δ_0 and the modification factor A.

$$
\begin{aligned}
{}^{e}\sigma_r - {}^{e}\sigma_\theta &= \frac{2YA\lambda}{\pi}\left[2(\delta-\delta_0)\right]^{-\frac{1}{2}}\left[\left(\frac{3}{4}-2\nu\right)\cos\frac{\psi}{2}\right. \\
&\quad \left. + \frac{1}{4}\cos\frac{5\psi}{2}\right] \\
{}^{e}\sigma_\theta - {}^{e}\sigma_z &= \frac{2YA\lambda}{\pi}\left[2(\delta-\delta_0)\right]^{-\frac{1}{2}}\left[\left(2\nu-\frac{5}{4}\right)\cos\frac{\psi}{2}\right. \\
&\quad \left. + \frac{1}{4}\cos\frac{5\psi}{2}\right] \qquad (2.4.2) \\
{}^{e}\sigma_z - {}^{e}\sigma_r &= \frac{2YA\lambda}{\pi}\left[2(\delta-\delta_0)\right]^{-\frac{1}{2}}\left[\frac{1}{2}\cos\frac{\psi}{2}-\frac{1}{2}\cos\frac{5\psi}{2}\right] \\
{}^{e}\tau_{zr} &= \frac{2YA\lambda}{\pi}\left[2(\delta-\delta_0)\right]^{-\frac{1}{2}}\left(\frac{1}{2}\sin\psi\cos\frac{3\psi}{2}\right) \\
{}^{e}\tau_{r\theta} &= {}^{e}\tau_{\theta z} = 0
\end{aligned}
$$

For a better comparison, the third deviatoric component has been plotted in Figure 7.

2.5. Matching the Elastic and Plastic Stresses at the Elastic-Plastic Boundary

To check the elastic and plastic stresses just derived, let us investigate the stresses in both regions as given by equations (2.3.1)

and (2.3.7a). At the elastic-plastic boundary $\delta_* = \delta_*(\psi)$, the stresses evaluated should of course satisfy the matching condition, namely,

$$ {}^{e}\sigma_{ij} \Big|_{\delta = \delta_*} = {}^{p}\sigma_{ij} \Big|_{\delta = \delta_*} \tag{2.5.1} $$

Analytically, we may investigate the elastic stress intensity

$$ {}^{e}\sigma_i = \frac{1}{\sqrt{2}} \left[({}^{e}\sigma_r - {}^{e}\sigma_\theta)^2 + ({}^{e}\sigma_\theta - {}^{e}\sigma_z)^2 + ({}^{e}\sigma_z - {}^{e}\sigma_r)^2 \right. $$

$$ \left. + 6\,({}^{e}\tau_{r\theta}{}^2 + {}^{e}\tau_{\theta z}{}^2 + {}^{e}\tau_{zr}{}^2) \right]^{\frac{1}{2}} \tag{2.5.2} $$

After substituting the values for elastic stresses from equations (2.3.1), we have the final elastic stress intensity

$$ {}^{e}\sigma_i = \frac{YA\lambda}{\pi} \left[2(\delta - \delta_o) \right]^{-\frac{1}{2}} m(\psi) \tag{2.5.3} $$

According to the yielding criterion in the theory of plasticity, this stress intensity should reach the yield stress Y when $\delta = \delta_*$, that is

$$ {}^{e}\sigma_i \Big|_{\delta = \delta_*} = Y \tag{2.5.4} $$

The combination of equations (2.5.3) and (2.5.4) gives

$$ Y = \frac{YA\lambda}{\pi} \left[2(\delta_* - \delta_o) \right]^{-\frac{1}{2}} m(\psi) \tag{2.5.5} $$

Solving this equation for δ_*, we have

$$\delta_* = \delta_o + \frac{1}{2}\left[\frac{A\lambda}{\pi} m(\psi)\right]^2 \tag{2.5.6}$$

This is the sought-for relation for the elastic-plastic boundary. However, the crack tip shifting distance enters here as a yet unknown function.

On the other hand, the plastic stress intensity of the Huber-Mises-Hencky's yielding criterion in equation (2.3.5) can be derived in the form of

$$^{p}\sigma_i = Y = \frac{AK}{\sqrt{2\phi}\,\delta^{\beta}}\left[(R-\theta)^2 + (\theta - Z)^2 + (Z-R)^2 + 6\,(ZR)^2\right]^{\frac{1}{2}} = \frac{2AK}{\phi\,\delta^{\beta}}\, m(\psi) \tag{2.5.7}$$

Solving for the generalized modulus of plastic deformation, we obtain

$$\phi = \frac{2AK}{Y\delta^{\beta}}\, m(\psi) \tag{2.5.8}$$

Recalling that the generalized modulus from equation (2.3.4) is a constant along the boundary, we rewrite (2.5.8) as follows

$$\phi\Big|_{\delta=\delta_*} = \frac{1}{2G} = \frac{2AK}{Y\,\delta_*^{\beta}}\, m(\psi) \tag{2.5.9}$$

This is the additional relationship defining δ_*. Substituting equation (2.5.6) into equation (2.5.9), we have

$$\frac{1}{2G} = \frac{2\Lambda K\, m(\psi)}{Y \left\{ \delta_o + \frac{1}{2} \left[\frac{\Lambda\lambda}{\pi} m(\psi) \right]^2 \right\}^{\beta}} \qquad (2.5.10)$$

which we can solve for the crack shifting distance δ_o

$$\delta_o = \left[\frac{A\lambda}{\pi} m(\psi) \right]^{1/\beta} - \frac{1}{2} \left[\frac{A\lambda}{\pi} m(\psi) \right]^2 \qquad (2.5.11)$$

By substituting the value of δ_o from equation (2.5.11) back to equation (2.5.6), we end up with the final expression for δ_*

$$\delta_* = \left[\frac{A\lambda}{\pi} m(\psi) \right]^{1/\beta} \qquad (2.5.12)$$

and for $\beta = \frac{1}{2}$,

$$\delta_* = \left[\frac{A\lambda}{\pi} m(\psi) \right]^2 \qquad (2.5.12a)$$

With the value of δ_* as in equation (2.5.12a), we may match the derived stresses in equations (2.4.1) and equations (2.4.7). Noting the strength singularity $\beta = \frac{1}{2}$, it can be verified that along the boundary $\delta = \delta_*$, the elastic stresses are identical to the plastic stresses, namely

$$ {}^{e}\sigma_r \Big|_{\delta = \delta_*} = {}^{p}\sigma_r \Big|_{\delta = \delta_*} = \frac{2Y}{m(\psi)} \left(\frac{3}{4} \cos\frac{\psi}{2} + \frac{1}{4} \cos\frac{5\psi}{2} \right) \qquad (2.5.13)$$

$$ {}^{e}\sigma_\theta \Big|_{\delta = \delta_*} = {}^{p}\sigma_\theta \Big|_{\delta = \delta_*} = \frac{4\nu Y}{m(\psi)} \cos\frac{\psi}{2} \qquad (2.5.14)$$

$$ {}^{e}\sigma_z \Big|_{\delta = \delta_*} = {}^{p}\sigma_z \Big|_{\delta = \delta_*} = \frac{2Y}{m(\psi)} \left(\frac{5}{4} \cos \frac{\psi}{2} - \frac{1}{4} \cos \frac{5\psi}{2} \right) \tag{2.5.15} $$

$$ {}^{e}\tau_{rz} \Big|_{\delta = \delta_*} = {}^{p}\tau_{rz} \Big|_{\delta = \delta_*} = \frac{Y}{m(\psi)} \sin \psi \cos \frac{3\psi}{2} \tag{2.5.16} $$

Also, the mean stress which is defined as

$$ \begin{aligned} {}^{e}\sigma_m &= \frac{1}{3} \left({}^{e}\sigma_r + {}^{e}\sigma_\theta + {}^{e}\sigma_z \right) \\ {}^{p}\sigma_m &= \frac{1}{3} \left({}^{p}\sigma_r + {}^{p}\sigma_\theta + {}^{p}\sigma_z \right) \end{aligned} \tag{2.5.17} $$

can be shown to match along the boundary:

$$ {}^{e}\sigma_m \Big|_{\delta = \delta_*} = {}^{p}\sigma_m \Big|_{\delta = \delta_*} = \frac{4Y(1+\nu)}{3\, m(\psi)} \cos \frac{\psi}{2} \tag{2.5.18} $$

Here the values of $m(\psi)$ and δ_* are given by equations (2.3.7b) and (2.5.12a), respectively.

To complete this section, the distributions of these common stress components along the elastic-plastic boundary are illustrated in Figures 8, 9, 10, 11 and 12.

2.6. Stress Analysis Based on the Maximum Principal Stress Criterion

After finishing the stress and strain analyses in this chapter through the Huber-Mises-Hencky criterion, we shall include the method

of finding stress components based on the maximum principal stress. According to earlier researchers, the Huber-Mises-Hencky criterion works well for metals however the maximum principal stress criterion may be justified better for solids exhibiting a fiber-like structure as for instance high-linear polymers.

In order to find the principal stresses, we have to find the roots of the following cubic equation

$$\begin{vmatrix} \sigma-\sigma_r, & 0, & \tau_{rz} \\ 0, & \sigma-\sigma_\theta, & 0 \\ \tau_{zr}, & 0, & \sigma-\sigma_z \end{vmatrix} = 0 \qquad (2.6.1)$$

The roots are found to be

$$\left.\begin{matrix} \sigma_\theta \\ \frac{\sigma_r+\sigma_z}{2} \pm \left[\left(\frac{\sigma_r-\sigma_z}{2}\right)^2+\tau_{rz}^2\right]^{\frac{1}{2}} \end{matrix}\right\} \qquad (2.6.2)$$

Let us denote the largest root of the equation (2.6.2) as σ_1, therefore

$$\sigma_1 = \frac{\sigma_r+\sigma_z}{2} + \left[\left(\frac{\sigma_r-\sigma_z}{2}\right)^2+\tau_{rz}^2\right]^{\frac{1}{2}} \qquad (2.6.3)$$

By substituting the elastic stress components from equation (2.3.1) into (2.6.3), and denoting it as ${}^e\sigma_1$, we have

$$ {}^{e}\sigma_1 = \frac{YA\lambda}{\pi} \left[2(\delta - \delta_o) \right]^{-\frac{1}{2}} \left(2 \cos \frac{\psi}{2} + \sin \psi \right) \qquad (2.6.4) $$

Equating equation (2.6.4) to a positive constant multiple of the yielding stress, αY, along the elastic-plastic boundary, that is

$$ {}^{e}\sigma_1 \Big|_{\delta = \delta_*} = \alpha Y \qquad (2.6.5) $$

and solving for δ_*, we get

$$ \left[2(\delta_* - \delta_o) \right]^{\frac{1}{2}} = \left(\frac{A\lambda}{\pi\alpha} \right) \left(\cos \frac{\psi}{2} + \sin \psi \right) \qquad (2.6.6) $$

The plastic stress field is obtained by substituting equation (2.6.6) into the elastic stress distribution given by equation (2.3.1). The final forms are

$$ \left.
\begin{aligned}
{}^{p}\sigma_r &= \frac{2Y}{\alpha} \cdot \frac{\frac{3}{4} \cos\frac{\psi}{2} + \frac{1}{4} \cos \frac{5\psi}{2}}{\cos \frac{\psi}{2} + \sin \psi} \\
{}^{p}\sigma_\theta &= \frac{2Y}{\alpha} \cdot \frac{2\nu \cos \frac{\psi}{2}}{\cos \frac{\psi}{2} + \sin \psi} \\
{}^{p}\sigma_z &= \frac{2Y}{\alpha} \cdot \frac{\frac{5}{4} \cos \frac{\psi}{2} - \frac{1}{4} \cos \frac{5\psi}{2}}{\cos \frac{\psi}{2} + \sin \psi} \\
{}^{p}\tau_{zr} &= \frac{2Y}{\alpha} \cdot \frac{\frac{1}{2} \sin \psi \cos \frac{3\psi}{2}}{\cos \frac{\psi}{2} + \sin \psi}
\end{aligned}
\right\} \qquad (2.6.7) $$

$$ {}^{p}\tau_{r\theta} = {}^{p}\tau_{\theta z} = 0 $$

The plastic stress distributions in equations (2.6.7) are plotted in Figures 13, 14 and 15.

Figure 16 illustrates the comparison between the stress distribution for the pure elastic range and for the elastic-plastic range as it results from the maximum principal stress criterion. It has been shown that the maximum principal stress criterion works better in polymers where the density change at the fracture front is considerable due to the crazing process. The crazing process is governed by σ_1.

CHAPTER III

INVESTIGATION OF CRACK TIP SHIFTING DISTANCE, ELASTIC-PLASTIC BOUNDARY AND STRENGTH SINGULARITY

In this chapter the equations for the crack shifting distance δ_0, elastic-plastic boundary δ_* and strength singularity β are derived and discussed.

3.1. Derivation of Crack Shifting Distance and Elastic-Plastic Boundary for the Case of $\beta = \frac{1}{2}$.

Recalling equation (2.5.11), we see that the distance δ_0 is a function of angle ψ and strength singularity β, that is

$$\delta_0 = \delta_0(\psi, \beta) \tag{3.1.1}$$

The full expression for δ_0 is

$$\delta_0(\psi, \beta) = \left[\frac{A\lambda}{\pi} m(\psi)\right]^{1/\beta} - \frac{1}{2}\left[\frac{A\lambda}{\pi} m(\psi)\right]^2 \tag{3.1.2}$$

Let us investigate the value of the crack shifting distance δ_0 at the lower value of $\beta = \frac{1}{2}$, i.e. for a quasi-brittle material. Thus

$$\delta_0(\psi, \tfrac{1}{2}) = \frac{1}{2}\left[\frac{A\lambda}{\pi} m(\psi)\right]^2 \tag{3.1.3}$$

and from equation (2.5.12a), we have

$$\delta_*(\psi, \tfrac{1}{2}) = \left[\frac{A\lambda}{\pi} m(\psi)\right]^2 \tag{3.1.4}$$

After comparing equations (3.1.3) and (3.1.4), we have

$$\delta_0(\psi,\tfrac{1}{2}) = \frac{1}{2}\,\delta_*(\psi,\tfrac{1}{2}) \tag{3.1.5}$$

This means that in the case of $\beta = \frac{1}{2}$, the crack shifting distance is one half of the critical distance measured from the crack tip to the elastic-plastic boundary. The result we have arrived at in this section agrees well with earlier observations by Hult and McClintock [22] and J. Rice [19].

3.2. Derivation of Crack Shifting Distance and Elastic-Plastic Boundary for the Case of $\beta = 1$.

A more justified value of β, at least for an ideally elastic-plastic solid is $\beta = 1$. The derivations and discussion are presented in this section.

From equation (3.1.2), for $\beta = 1$, we have the shifting distance

$$\delta_0(\psi,1) = \left[\frac{A\lambda}{\pi}\, m(\psi)\right] - \frac{1}{2}\left[\frac{A\lambda}{\pi}\, m(\psi)\right]^2 \tag{3.2.1}$$

and from equation (2.5.12), for $\beta = 1$, we get the elastic-plastic boundary as

$$\delta_*(\psi,1) = \frac{A\lambda}{\pi}\, m(\psi) \tag{3.2.2}$$

3.3. Plots and Discussion of General Results

The graphical representation of the crack shifting distance δ_0 and elastic-plastic boundary δ_* for the cases of $\beta = \frac{1}{2}$ and $\beta = 1$

are given in Figure 17 and Figures 18, 19, 20, respectively. Let us summarize here the important results of this chapter.

$$\delta_* - \delta_o = \frac{1}{2}\left[\frac{A\lambda}{\pi} m(\psi)\right]^2 \qquad (3.3.1)$$

and

$$\delta_* = \left[\frac{A\lambda}{\pi} m(\psi)\right]^{1/\beta} \qquad (3.3.2)$$

With equations (3.3.1) and (3.3.2), we conclude now that

$$\delta_* - \delta_o = \frac{1}{2}\delta_*^{2\beta}$$

or

$$\delta_o = \delta_* - \frac{1}{2}\delta_*^{2\beta} \qquad (3.3.4)$$

This relates the crack tip shifting distance to the dimension of the elastic-plastic boundary for any given value of the strength singularity β.

It is seen that in the case of $\beta = \frac{1}{2}$, equation (3.3.4) will give the same result as equation (3.1.5), that is

$$\delta_o = \frac{1}{2}\delta_* \qquad (3.3.5)$$

In the case of $\beta = 1$, equation (3.3.4) gives the same value as equation (3.2.1) or

$$\delta_o = \delta_* - \frac{1}{2}\delta_*^2 \qquad (3.3.6)$$

As we mentioned in Chapter II, the strength of the singularity may vary in the interval of $\frac{1}{2} \leq \beta \leq 1$, the lower value being appropriate for high strain hardening, while β approaches unity for zero strain hardening (see Hutchinson [21]).

Since δ_*^e is small compared to δ_*, we can conclude that the crack tip shifting distance δ_o changes from about half of the plastic zone size when $\beta = \frac{1}{2}$ to almost full value of the plastic zone dimension when $\beta = 1$.

All the intermediate values of the strength singularity will lead to a crack tip shifting distance enclosed within the interval

$$\frac{1}{2}\delta_* \leq \delta_o \leq \delta_* \qquad (3.3.7)$$

CHAPTER IV

INVESTIGATION OF THE ELASTIC-PLASTIC MODIFICATION FACTOR

The modification factor "A" is determined by the application of the minimum potential energy principle. It is found that the value of factor "A" depends on λ, i.e. the ratio of load to yield stress; it is also shown that when λ tends to zero, the factor "A" tends to unity which agrees with the result obtained by Sneddon for a purely elastic solid.

4.1. Evaluation of Energy Densities

The total strain energy of an ideally homogenous, isotropic and elastic-plastic material can be expressed in the following form:

$$\text{Total Strain Energy} = (\text{Total Elastic Energy}) + (\text{Total Plastic Energy}) \tag{4.1.1}$$

Or expressed in terms of energy components,

$$\text{Total Strain Energy} = \big[(\text{Elastic Energy of Whole Region}) - (\text{Elastic Energy in Plastic Region})\big] + (\text{Total Plastic Energy in Plastic Region}) \tag{4.1.2}$$

Mathematically,

$$U = U_e + U_p \tag{4.1.3}$$

or in terms of energy components,

$$U = \left[\int_{V=-\infty}^{+\infty} ({}^{e}u_v + {}^{e}u_f)\, dV - \int_{V_p} ({}^{e}u_v + {}^{e}u_f)\, dV\right] + \left[\int_{V_p} ({}^{p}u_v + {}^{p}u_f)\, dV\right] \tag{4.1.4}$$

where, from [23], the volume energy density u_v and the distortional energy density u_f in the elastic and plastic regions are given by the following relations

$$\left.\begin{aligned} {}^{e}u_v &= \frac{3(1-2\nu)}{2E}\left(\frac{{}^{e}\sigma_r + {}^{e}\sigma_\theta + {}^{e}\sigma_z}{3}\right)^2 \\ {}^{e}u_f &= \frac{2(1+\nu)}{3}\cdot\frac{{}^{e}\sigma_i{}^2}{2E} \end{aligned}\right\} \tag{4.1.5}$$

$$\left.\begin{aligned} {}^{p}u_v &= \frac{3(1-2\nu)}{2E}\left(\frac{{}^{p}\sigma_r + {}^{p}\sigma_\theta + {}^{p}\sigma_z}{3}\right)^2 \\ {}^{p}u_f &= \frac{2(1+\nu)}{3}\left({}^{Y}{}^{p}\epsilon_i - \frac{Y^2}{2E}\right) \end{aligned}\right\} \tag{4.1.6}$$

where the elastic stress intensity and plastic strain intensity are defined as

$${}^{e}\sigma_i = \frac{1}{\sqrt{2}}\left[({}^{e}\sigma_r - {}^{e}\sigma_\theta)^2 + ({}^{e}\sigma_\theta - {}^{e}\sigma_z)^2 + ({}^{e}\sigma_z - {}^{e}\sigma_r)^2 + 6\,({}^{e}\tau_{r\theta}^2 + {}^{e}\tau_{\theta z}^2 + {}^{e}\tau_{rz}^2)\right]^{\frac{1}{2}} \tag{4.1.7}$$

$${}^{p}\epsilon_i = \frac{1}{\sqrt{2}(1+\nu)}\left[({}^{p}\epsilon_r - {}^{p}\epsilon_\theta)^2 + ({}^{p}\epsilon_\theta - {}^{p}\epsilon_z)^2 + ({}^{p}\epsilon_z - {}^{p}\epsilon_r)^2 + \frac{3}{2}({}^{p}\gamma_{r\theta}^2 + {}^{p}\gamma_{zr}^2 + {}^{p}\gamma_{\theta z}^2)\right] \tag{4.1.8}$$

Equation (4.1.4) is an exact expression for the energy relation; however, we may simplify this equation by proper physical interpretation.

First, the elastic energy of the whole region in Sneddon's solution was

$$U_o = \int_{-\infty}^{+\infty} {}^{o}u \, dV = \frac{8(1-\nu^2)\, L^3\, P^2}{3E} \qquad (4.1.9)$$

For our case, we sh. ld put the proper half crack length as the sum of L and the reduced shifting distance (see Appendix II), and replace P_o by the product (AP_o). Therefore the reduced elastic energy becomes

$$U_{red} = A^2 \frac{8(1-\nu^2)\, (L + L\, \delta_{red})^3\, P_o^2}{3E}$$

$$\cong U_o\, (1 + 3\, \delta_{red}) \qquad (4.1.10)$$

where the reduced crack tip shifting distance δ_{red} is derived in Appendix II.

Second, we have shown that the total elastic energy consists of two parts, the elastic energy of the whole region and the elastic energy in the plastic region. However, under practical conditions, the component of the elastic energy in the plastic region is relatively small and negligible compared to the elastic energy of the whole region. Hence we may conclude that the total elastic energy is represented by the reduced elastic energy

$$U_e = U_{red} \qquad (4.1.11)$$

Similarly, in dealing with the total plastic energy in the plastic region, the distortional part of energy is much more effective than the volume energy component. After neglecting the volume energy component, we have

$$U_p \overset{\infty}{=} \int_{V_p} {}^{p}u_r \, dV \tag{4.1.12}$$

Finally, the total energy in equation (4.1.4) is reduced to

$$U = U_e + U_p = U_{red} + \int_{V_p} {}^{p}u_f \, dV \tag{4.1.13}$$

It is noticed that neglecting the reduction of elastic energy in the plastic region will tend to increase the total energy in equation (4.1.4); however, neglecting the addition of the volume energy component will decrease the total energy. Therefore, it is believed that due to the mutual compensation of these neglected parts, the result in equation (4.1.13) is a reasonable approximation.

The plastic energy in equation (4.1.12) can be evaluated from integration in the whole plastic region. The distorsional plastic energy density can be obtained from (4.1.6); therefore

$$\begin{aligned} U_p &\overset{\infty}{=} \int_{V_p} {}^{p}u_f \, dV \\ &= \int_{V_p} \frac{2(1+\nu)}{3} \left(Y \, {}^{p}\epsilon_i - \frac{Y^2}{2E} \right) dV \end{aligned} \tag{4.1.14}$$

The plastic strain intensity is taken from equation (4.1.8),

$$ {}^{p}\epsilon_i = \frac{1}{\sqrt{2}(1+\nu)} \left[({}^{p}\epsilon_r - {}^{p}\epsilon_\theta)^2 + ({}^{p}\epsilon_\theta - {}^{p}\epsilon_z)^2 + ({}^{p}\epsilon_z - {}^{p}\epsilon_r)^2 \right. $$

$$ \left. + \frac{3}{2} ({}^{p}\gamma_{r\theta}^2 + {}^{p}\gamma_{zr}^2 + {}^{p}\gamma_{\theta z}^2) \right]^{\frac{1}{2}} $$

After substituting strain components from (2.2.2), we have

$$ {}^{p}\epsilon_i = \frac{AK}{\sqrt{2}(1+\nu)\,\delta^\beta} \left[(R-\theta)^2 + (\theta-Z)^2 + (Z-R)^2 + \frac{3}{2} ZR^2 \right]^{\frac{1}{2}} $$

The angular functions are obtained from equations (2.1.5); hence the final plastic strain intensity is given by

$$ {}^{p}\epsilon_i = \frac{2AK}{(1+\nu)\,\delta^\beta} \left[3 \sin^2\psi + 4(1-2\nu)^2 \cos^2\frac{\psi}{2} \right]^{\frac{1}{2}} \qquad (4.1.15) $$

or using the shortened notation, we have

$$ {}^{p}\epsilon_i = \frac{YA\lambda}{\pi E} \left(\frac{1}{\delta}\right)^\beta m(\psi) \qquad (4.1.15a) $$

The differential volume as shown in Figure 21 is

$$ dV = 2\pi (L + \delta_1 \cos\psi)\, \delta_1\, d\delta_1\, d\psi $$

where $\delta_1 = L\delta$

and the integration limits are

$$ 0 \le \delta_1 \le \delta_{1_*}(\psi) $$

$$ 0 \le \psi \le 2\pi $$

Hence, the integration in equation (4.1.14) becomes

$$U_p = \int_0^{2\pi} \int_0^{\delta_*} \frac{Y^2(1+\nu)}{3E} \left[\frac{2A\lambda}{\pi} \left(\frac{L}{\delta_1} \right)^{\beta} m(\psi) - 1 \right] \cdot (L + \delta_1 \cos\psi) \cdot 2\pi \delta_1 \, d\delta_1 \, d\psi \qquad (4.1.16)$$

A brief summary of equations for evaluating energy components is presented here for convenience of further derivation:

$$\left.\begin{aligned} U_o &= \frac{8(1-\nu^2) L^3 P_o^2}{3E} \\ U_e &= U_o A^2 (1 + 3\delta_{red}) \\ U_p &= \int_0^{2\pi} \int_0^{\delta_*} \frac{Y^2(1+\nu)}{3E} \left[\frac{2A\lambda}{\pi} \left(\frac{L}{\delta_1} \right)^{\beta} m(\psi) - 1 \right] \cdot \\ &\quad (L + \delta_1 \cos\psi) \cdot 2\pi \delta_1 \, d\delta_1 \, d\psi \end{aligned}\right\} \qquad (4.1.17)$$

4.2. Application of Principle of Minimum Potential Energy

As in the theory of elasticity [23], the potential energy Π of the system is defined as

$$\Pi = U - W \qquad (4.2.1)$$

where U is the potential energy of deformation and -W represents the potential energy of the external forces acting on the body if the potential energy of these forces for the unstressed condition is taken to be zero.

The principle of minimum potential energy states that, "the stable equilibrium state of a system is that for which the potential

energy of the system attains the minimum", i.e. the first variation of Π vanishes:

$$\delta \Pi = \delta (U - W) = 0 \qquad (4.2.2)$$

The operator "δ" means partial differentiation with respect to the assumed system parameters.

Before we apply the principle of potential energy, as given by equation (4.2.2), the potential energy of deformation U must be evaluated from equations (4.1.17); the change in potential energy of external forces is evaluated as

$$W = \int_S T_i \, u_i \, dS \qquad (4.2.3)$$

where T_i are the tractions applied to the surface of the solid, u_i is the kinematically admissible displacement field, and S denotes the part of the body surface on which the forces T_i are applied.

Equation (4.2.3) can also be written in an expanded form as

$$W = \int_S (T_r \, u_r + T_\theta \, u_\theta + T_z \, u_z) \, dS \qquad (4.2.4)$$

For our loading condition

$$T_r = T_\theta = 0, \quad T_z = P_0$$

and

$$u_z \neq 0, \quad u_r = u_\theta = 0 \text{ for } z = 0$$

then equation (4.2.4) becomes

$$W = \int_S P_o \, u_z \, dS \qquad (4.2.5)$$

where $dS = 2\pi \, r dr$; thus

$$W = 2\pi \int_0^L P_o \, u_z \, r dr \qquad (4.2.5a)$$

4.3. Evaluation of the Factor "A" for Quasi-brittle Solids

The value of the amplitude "A" for brittle solids, i.e. $\beta = \frac{1}{2}$, is evaluated in this section by applying the minimum potential energy principle as discussed in the previous section.

From equations (4.1.17), the elastic energy is

$$U_e = A^2 \, U_o \, (1 + 3 \, \delta_{red})$$

where the reduced crack shifting distance we have from the Appendix II is

$$\delta_{red}\left(\beta = \tfrac{1}{2}\right) = \frac{3\sqrt{3}\, H^{\frac{1}{2}}(\nu)}{2\sqrt{2}\,\pi^2} \, A^2 \, \lambda^2$$

Therefore the elastic energy is

$$U_e \left(\beta = \tfrac{1}{2}\right) = A^2 \, U_o \, (1 + C_1 \, A^2 \, \lambda^2) \qquad (4.3.1)$$

where

$$U_o = \frac{8(1-\nu^2) \, L^3 \, P_o^{\,2}}{3E}$$

$$C_1 = \frac{9\sqrt{3}\, H^{\frac{1}{2}}(\nu)}{2\sqrt{2}\,\pi^2}$$

$$H(\nu) = 1 + \frac{16}{9}(1-2\nu)^2 + \frac{16}{9}(1-2\nu)^4 \qquad \Big\} \quad (4.3.1a)$$

The total plastic energy as given by equation (4.1.17) is

$$U_p = \int_0^{2\pi}\int_0^{\delta_{1*}} \frac{Y^2(1+\nu)}{3E}\left[\frac{2A\lambda}{\pi}\left(\frac{L}{\delta_1}\right)^{\beta} m(\psi) - 1\right] \cdot (L + \delta_1 \cos\psi)\cdot 2\pi\,\delta_1\, d\delta_1\, d\psi$$

After integrating with respect to δ_1, we get

$$U_p\ (\beta = \tfrac{1}{2}) = \frac{2\pi L Y^2(1+\nu)}{3E}\left(\frac{4A\lambda L^{\frac{1}{2}}}{3\pi}\int_0^{2\pi} m(\psi)\cdot\delta_1^{3/2}\, d\psi - \tfrac{1}{2}\int_0^{2\pi}\delta_{1*}^2\, d\psi\right)$$

where the elastic-plastic boundary is given by equation (3.1.4), i.e.

$$\delta_{1*} = L\,\delta_* = \left(\frac{A\lambda}{\pi}\right)^2 L\, m^2(\psi)$$

After substituting and performing the integration, we have the final result as follows

$$U_p\ (\beta = \tfrac{1}{2}) = \frac{15(1+\nu)Y^2L^3}{4E\pi^2} H(\nu)\,(A\lambda)^4$$

In a shorter form,

$$U_p = C_3\, U_o\, A^4\, \lambda^2 \qquad (4.3.2)$$

Hence it is seen that the energy dissipated in the plastic zone is proportional to the fourth power of the load ratio. Also, $\lambda = P_o/Y$ since $u_o \propto \lambda^2$.

Symbols used in Equation (4.3.2) are

$$\left.\begin{aligned} U_o &= \frac{8(1-\nu^2)\, L^3 P_o^{\,2}}{3E} \\ C_3 &= \frac{45\, H(\nu)}{32\, \pi^2 (1-\nu)} \\ H(\nu) &= 1 + \frac{16}{9}(1-2\nu)^2 + \frac{16}{9}(1-2\nu)^4 \end{aligned}\right\} \quad (4.3.2a)$$

As we know the total strain energy is the sum of elastic and plastic energies, or

$$\begin{aligned} U &= U_e + U_p \\ &= U_o \left[A^2 + (C_1 + C_3)\, A^4 \lambda^2 \right] \end{aligned} \quad (4.3.3)$$

The potential energy attributed to the external forces may be obtained from equation (4.2.5a). However, instead of tedious integration we may apply the result of Sadeghi [24] that the external work is twice the elastic energy divided by A; therefore,

$$W = 2\,\frac{1}{A}\,U_e = U_o\,(2A + 2C_1\, A^3\, \lambda^2) \quad (4.3.4)$$

With equations (4.3.3) and (4.3.4) and from equation (4.2.2) we are ready to apply the principle of the minimum potential energy and finally to evaluate the factor "A".

Thus

$$\delta \Pi = \delta \left[(A^2 U_e + U_p) - 2A U_e \right] = 0 \qquad (4.3.5)$$

We substitute the elastic and plastic energy components and write equation (4.3.5) in an expanded form

$$\frac{\partial \Pi}{\partial A} = \frac{\partial}{\partial A} \left[U_o(A^2 + C_1 A^4 \tau^2 + C_3 A^4 \tau^2) - U_o (2A + 2C_1 A^3 \tau^2) \right]$$

$$= 0$$

After differentiation, we get

$$(A - 1) - 3C_1 \tau^2 A^2 + (2C_1 + 2C_3) \tau^2 A^3 = 0 \qquad (4.3.6)$$

This cubic equation we shall solve by approximation method. Let us express the sought-for factor A as a function of τ in the following way

$$\left.\begin{aligned} A &= 1 + A_1 \tau^2 + A^2 \tau^4 + \cdots \\ A^2 &= 1 + 2A_1 \tau^2 + (A_1^2 + 2A_2) \tau^4 + \cdots \\ A^3 &= 1 + 3A_1 \tau^2 + (3A_1^2 + 3A_2) \tau^4 + \cdots \end{aligned}\right\} \qquad (4.3.7)$$

Substituting (4.3.7) into (4.3.6) and neglecting the terms of order higher than τ^4, we get

$$(A_1 - C_1 + 2C_3) \tau^2 + (A_2 + 6C_3 A) \tau^4 = 0 \qquad (4.3.8)$$

Now, we solve for A_1 and A_2 by letting the coefficients of the terms λ^2 and λ^4 to be equal to zero, respectively. We have

$$\left.\begin{aligned} A_1 &= C_1 - 2C_3 \\ A_2 &= -6C_3 A_1 = -6C_1 C_3 + 12 C_3^2 \end{aligned}\right\} \quad (4.3.9)$$

where the constants are

$$\left.\begin{aligned} C_1 &= \frac{9\sqrt{3}\, H^{\frac{1}{2}}(\nu)}{2\sqrt{2}\,\pi^2} \\ C_3 &= \frac{45\, H(\nu)}{32\,\pi^2 (1-\nu)} \\ H(\nu) &= 1 + \frac{16}{9}(1-2\nu)^2 + \frac{16}{9}(1-2\nu)^4 \end{aligned}\right\} \quad (4.3.9a)$$

The final expression for the modification factor in the case of $\beta = \frac{1}{2}$ has the following form

$$A = 1 + \left[\frac{9\sqrt{3}\, H^{1/2}(\nu)}{2\sqrt{2}\,\pi^2} \quad \frac{45\, H(\nu)}{16\pi^2 (1-\nu)}\right] \lambda^2 - \frac{135\, H(\nu)}{16\,\pi^2 (1-\nu)} \left[\frac{9\sqrt{3}\, H^{1/2}(\nu)}{2\sqrt{2}\,\pi^2} - \frac{45\, H(\nu)}{16\,\pi^2 (1-\nu)}\right] \lambda^4 + \ldots \quad (4.3.10)$$

To be more specific, let us consider two extreme cases:

a) For an incompressible solid, $\nu = \frac{1}{2}$; then equation (4.3.10) gives

$$A = 1 - 0.011\, \lambda^2 + 0.018\, \lambda^4 + \ldots$$

b) For $\nu = 0$, we have

$$A = 1 - 0.097\, \lambda^2 + 0.372\, \lambda^4 + \ldots$$

From the general solution in equation (4.3.10), it is found that the value of the factor A is a function of the ratio of load to yield stress and the Poisson ratio. Whenever λ tends to zero, the value of A is unite which agrees with the result of Sneddon. The correction terms appearing in (4.3.10) are small, therefore it may be concluded that the major influence of the plastic zone on the stress distribution around the fracture front can be attributed to the crack tip shifting distance, as discussed earlier.

CHAPTER V

MODIFICATION OF FRACTURE CRITERION

Because of different approaches in evaluating the energy components in the very vicinity of the crack tip, we may expect different results for the critical stress opening the crack. A new value for the critical stress at which the crack will start to propagate is obtained from a modified fracture criterion. Our result is comparable to the Griffith-Irwin criterion for large cracks, but it deviates considerably from the classical solution in the range of crack length close to the "characteristic" length. The latter is found to be proportional to the square of the ratio of the critical K-factor to the yield stress Y.

5.1. The Energy Balance at the Crack Tip

The explanation of a fracture on the basis of the energy balance of a cracked body was given by Griffith. Irwin arrived at the same fracture criterion through the calculation of the work done locally at the crack tip during a small virtual increase in crack length.

We shall now consider Irwin's approach and make use of the energy components in Chapter IV. Let us investigate the effects of a small, virtual change of the crack tip position ΔL. The elastic-plastic region at the crack tip will undergo a small distortion and the forces acting on it will do work. There will be a certain amount of the external work ΔW which can be evaluated from equation (4.3.4).

A certain amount of this dissipated work is transformed into another form of free energy. This portion of energy will be called SE, or surface energy which is necessary to create the new surface. The remaining energy is stored as the strain energy U_e or dissipated as the plastic work U_p within the plastic region. The whole process is assumed to take place slowly and isothermally, so that the involved kinetic energy and other possible sources of energy dissipation are small and negligible.

From the first law of thermodynamics, the energy balance can be expressed in the following incremental form

$$\Delta_L W = \Delta_L U + \Delta_L SE \qquad (5.1.1)$$

where Δ_L denotes the differential operator $\frac{\partial}{\partial L}$.

5.2. Evaluation of Energy Components

The incremental form of equation (5.1.1) can be written in the form of partial differentiation as

$$\frac{\partial W}{\partial L} = \frac{\partial U}{\partial L} + \frac{\partial SE}{\partial L} \qquad (5.2.1)$$

The component of external work can be obtained from equation (4.3.4), and we have

$$W \cong 2\left(\frac{1}{A}\right) U_e = 2A\, U_o \qquad (5.2.2)$$

The total energy of the elastic and plastic regions is given by equation (4.1.13),

$$U \cong U_{red} + \int_{V_p} p u_f \, dV \tag{5.2.3}$$

The surface energy is defined as the product of the area and the specific energy. Mathematically,

$$SE = 2\pi\gamma L^2 \tag{5.2.4}$$

where L is the half crack length, γ denotes the specific surface energy and the factor 2 exists due to symmetry.

5.3. Modified Fracture Criterion for Quasi-brittle Solids

A modified fracture criterion will be derived for quasi-brittle solids, i.e. for $\beta = \frac{1}{2}$. The generalized energy balance equation is used to generate the criterion.

By substituting equations (5.2.4), (5.2.2) and (5.2.3) into equation (5.2.1), we have

$$\frac{\partial}{\partial L}(W - U_e - U_p) = \frac{\partial}{\partial L} SE \tag{5.3.1}$$

Or substituting the expanded forms from equations (4.3.1), (4.3.2) and (4.3.4), equation (5.3.1) becomes

$$(2A + 2C_1 A^3 \lambda^2 - A^2 - C_1 A^4 \lambda^2 - C_3 A^4 \lambda^2) \frac{\partial}{\partial L} U = \frac{\partial}{\partial L} SE$$

After performing the differentiation, we have

$$\left[(2A - A^2) + (2C_1 A^3 - C_1 A^4 - C_3 A^4) \lambda^2 \right] \cdot \frac{8(1-\nu^2)L^2}{E} P_o^2 = 4 \pi \gamma L$$

This we can solve for the critical stress

$$P_o = \frac{1}{\sqrt{(2A-A^2) + (2C_1 A^3 - C_1 A^4 - C_3 A)\lambda^2}} \cdot \left[\frac{\pi E \gamma}{2(1-\nu^2)L} \right]^{\frac{1}{2}} \qquad (5.3.2)$$

It should be noted, however, that P_o is also implicit in the dimensionless load λ. We shall therefore proceed to resolve (5.3.2) with respect to P_o. We recognize $\left[\frac{\pi E \gamma}{2(1-\nu^2)L} \right]^{\frac{1}{2}}$ as Griffith critical stress P_G. For small λ, the square root

$$\left[(2A - A^2) + (2C_1 A^3 - C_1 A^4 - C_3 A^4) \lambda^2 \right]^{-\frac{1}{2}}$$

can be expanded if we recall that the following relations are true for the factor A

$$A = 1 + A_1 \lambda^2 + A_2 \lambda^4 + \cdots$$

$$A^2 = 1 + 2A_1 \lambda^2 + (A_1^2 + 2A_2) \lambda^4 + \cdots$$

$$A^3 = 1 + 3A_1 \lambda^2 + (3A_1^2 + 3A) \lambda^4 + \cdots$$

$$A^4 = 1 + 4A_1 \lambda^2 + (6 A_1^2 + 4 A_2) \lambda^4 + \cdots$$

Grouping and neglecting the terms of order higher than λ^2, we get

$$\left[(2A - A^2) + (2C_1 A^3 - C_1 A^4 - C_3 A^4) \lambda^2 \right]^{-\frac{1}{2}}$$
$$= \left[1 + (C_1 - C_3) \lambda^2 + \cdots \right]^{-\frac{1}{2}}$$
$$= \left(1 - \frac{C_1 - C_3}{2} \lambda^2 + \cdots \right)$$

Let $\phi = C_1 - C_2$, then equation (5.3.2) becomes

$$P_o = \left(1 - \frac{\phi}{2} \lambda^2\right) P_G \qquad (5.3.3)$$

where

$$\phi = \left[\frac{9\sqrt{3}\, H^{\frac{1}{2}} (\nu)}{2\sqrt{2}\, \pi^2} - \frac{45\, H(\nu)}{32\, \pi^2 (1-\nu)} \right] \qquad (5.3.3a)$$

From equation (5.3.3), we will work out a curve of dimensionless critical load P_{crit}/Y versus dimensionless crack L/L_*.

Equation (5.3.3) can be written as

$$\lambda = \left(1 - \frac{\phi}{2} \lambda^2\right) \frac{P_G}{Y} \qquad (5.3.4)$$

which we solve with respect to λ. The solution

$$\lambda_{crit} = \frac{P_G}{Y} \left[1 - \frac{1}{2} \left(\frac{P_G}{Y}\right)^2 \phi \right] \qquad (5.3.5)$$

or simply

$$P_{crit} = P_G \left[1 - \frac{1}{2} \left(\frac{P_G}{Y}\right)^2 \phi \right] \qquad (5.3.6)$$

is the sought-for final expression for the critical load opening the crack. It is seen that for the vanishingly small ratios of P_G/Y, equation (5.3.5) reduces to the well-known Griffith-Sneddon-Sack formula. The correction factor

$$\frac{1}{2Y}\cdot\frac{\pi E\gamma}{2(1-\nu^2)L}\cdot\left[\frac{9\sqrt{3}H^{\frac{1}{2}}}{2\sqrt{2}\pi^2}-\frac{45H}{32\pi^2(1-\nu)}\right]$$

plays a significant role only for the crack length sufficiently small.

From Irwin [3] we may define the stress concentration factor K_c as

$$K_c = P_G\sqrt{\pi L}$$

Equation (5.3.6) becomes the

$$P_{crit} = P_G\left(1-\frac{\phi}{2\pi Y^2}\frac{K_c^2}{L}\right) \qquad (5.3.7)$$

If we introduce now a characteristic length

$$L_* = \frac{K_c^2}{2\pi Y^2}$$

then equation (5.3.7) gives

$$P_{crit} = P_G\left(1-\phi\frac{L_*}{L}\right) \qquad (5.3.8)$$

Similarly, it can be shown that

$$\frac{P_G}{Y} = \frac{(2L_*)^{\frac{1}{2}}}{L} \qquad (5.3.9)$$

By substituting equation (5.3.9) into (5.3.8) and denoting the dimensionless crack length by ζ, $\zeta = L/L_{x}$, we get

$$\frac{P_{crit}}{Y} = \sqrt{\frac{2}{\zeta}}\left(1 - \frac{\phi}{\zeta}\right) \tag{5.3.10}$$

where the value of ϕ is given by equation (5.3.3a). For $\nu = 0.3$ we have

$$\phi \Big|_{\nu = 0.3} = 0.373 \tag{5.3.10a}$$

The comparison of the result of equation (5.3.10) and the classical Griffith criterion is shown in Figure 22.

CHAPTER VI

CONCLUDING REMARKS

The essential points of this thesis may now be summarized as follows:

1. Engineering experience has demonstrated that most serious structure failures arise from unexpected extensions of pre-existing cracks or crack-like flaws. In practical applications the penny-shaped crack geometry can be considered whenever the flaws found inside the material or on the material surface have the form of a circular defect.
2. The results given in Chapter II describe the elastic and plastic analyses in an elastic-plastic solid containing an initial crack of 2L diameter. The Huber-Mises-Hencky plasticity condition has been employed to explain the ductile behavior of metals.
3. The stress analysis in section (2.6) based on the maximum principal stress criterion, is believed to be more justified for solids exhibiting a fiber-like structure such as high-linear (glass-like) polymers.
4. The mathematical infinite stress frequently referred to as the stress singularity at the crack tip is physically inadmissible. The idea of removing this singularity has been discussed in Chapter II. We did not completely succeed in removing the singularity in all cases; the quasi-brittle solid (for which

$\beta = \frac{1}{2}$) inherits the elastic type of singularity for the normal stresses, but the deviatoric components of the stress tensor are finite at the crack tip (see Figure 2). For an ideally elastic-plastic solid in which the plastic strains behave as $1/\delta$, where δ is the distance measured from the crack tip, we obtain a singularity-free stress distribution around the crack tip (see Figure 16).

5. Equation (3.3.3) and equation (3.3.4) are the derived formulae which govern the amount of crack tip shifting distance and the size of the elastic-plastic boundary.

6. It is found in Chapter IV, equation (4.3.10), that the value of the elastic-plastic modification factor "A" is a function of the ratio of load to yield stress (λ). Whenever the dimensionless load λ tends to zero, the value of "A" approaches unity which agrees with the classical result of Sneddon.

7. The modified critical stress precipitating a fracture as found in Chapter V is smaller than that given by Sack and Sneddon for a purely elastic solid. It compares well with the Irwin theory of fracture except for very small crack lengths at which the plastic energy dissipation becomes the dominant controlling factor.

8. This thesis discusses fracture in inelastic solids from the theoretical point of view. We believe intensive experimental evidence should be gathered before recommending our findings for the purpose of practical applications in specific engineering areas.

9. In general, the tensile crack toughness depends upon the amount of elastic constraint around the plastic zone. On the basis of fracture mechanics it can be said that a material would achieve optimum strength if it were fine in surface texture with coarse grain interior.

10. The practical goal of fracture mechanics is not only to prevent failure but also to raise the efficiency in the control of fabrication and quality control. A capability for optimization estimates which include fracture strength should be the ultimate goal. Therefore, the essential idea suggests that improvements in the fracture control require careful control of fabrication and repair procedures to mitigate such defects as weld and heat affected zone cracks and the development of brittle microstructures, and also various forms of mechanical damage during production, such as tool marks and gouges.

APPENDIX I

COEFFICIENT OF LATERAL DEFORMATION IN ELASTIC AND PLASTIC REGIONS

Since the coefficient of lateral deformation in elasticity, or Poisson's ratio is defined as

$$\nu = \frac{\text{Unit lateral contraction}}{\text{Unit axial elongation}}$$

or

$$\nu = \frac{-\epsilon(\text{lateral})}{\epsilon(\text{axial})}$$

we may define the coefficient of lateral deformation in the plastic region ν^1 in a similar way as

$$\nu^1 = \frac{-\epsilon(\text{lateral})}{\epsilon(\text{axial})}$$

Let us consider the case of a rod under uniaxial tension, σ_x. The corresponding strain will be ϵ_x, as shown in Figure 23, then the other strains are

$$\epsilon_y = -\nu^1 \epsilon_x$$

$$\epsilon_z = -\nu^1 \epsilon_x$$

Applying the dilational stress-strain relation

$$\epsilon_x + \epsilon_y + \epsilon_z = \frac{1-2\nu}{E} (\sigma_x - \sigma_y - \sigma_z)$$

substituting the stress and strain components, we obtain

$$\epsilon_x (1 - 2\nu') = \frac{1-2\nu}{E} \sigma_x$$

From this equation we may solve for the general form for the coefficient of lateral deformation as

$$\nu' = \frac{1}{2} - \frac{1-2\nu}{2E} \frac{\sigma_x}{\epsilon_x}$$

If the stressed rod is within elastic region we have the stress-strain relation from Hooke's law as

$$\sigma_x = E \epsilon_x$$

Then

$$\nu' = \frac{1}{2} - \frac{1-2\nu}{2} = \nu$$

This result checks with the definition of Poisson's ratio.

If the strain is large enough to be in the plastic region, from the Huber-Mises-Hencky yield criterion we get

$$^p\sigma_i = \sigma_x, \quad ^p\sigma_i = Y, \quad \sigma_x = Y$$

After substitution, we end up with the final form as

$$\nu' = \frac{1}{2} - \frac{1-2\nu}{2\epsilon_x}\left(\frac{Y}{E}\right)$$

This equation is plotted in Figure 23 by assuming $\nu = 0.3$, $\frac{Y}{E} = 10^{-3}$ for mild steel. The graph shows the conclusion "At large strains in the plastic region, an initially elastic solid tends to be incompressible, that is $\nu^1 \longrightarrow \frac{1}{2}$".

APPENDIX II

EVALUATION OF REDUCED CRACK TIP SHIFTING DISTANCE

The reduced crack tip shifting distance is defined as the diameter of a circle in which the area enclosed by the circle is equal to the area of the plastic region influenced by the real crack tip shifting distance.

The area enclosed by the circle of reduced crack tip shifting distance is

$$\text{AREA} = \frac{1}{4}\pi \delta_{red}^2 \tag{AII-1}$$

The area of the plastic region influenced by the real crack tip shifting distance is

$$\text{AREA} = \int_0^{2\pi} d\psi \cdot \int_0^{\delta_o(\psi)} \delta \, d\delta \tag{AII-2}$$

Equating equations (AII-1) and (AII-2) gives

$$\frac{1}{4}\pi \delta_{red}^2 = \int_0^{2\pi} d\psi \int_0^{\delta_o(\psi)} \delta \, d\delta \tag{AII-3}$$

From equation (AII-3), we solve for reduced crack tip shifting distance and have

$$\delta_{red} = \left(\frac{2}{\pi}\right)^{\frac{1}{2}} \left[\int_0^{2\pi} \delta_o^2(\psi) d\psi\right]^{\frac{1}{2}} \tag{AII-4}$$

Substituting δ_o from equation (3.1.3) and integrating equation (AII-4), we obtain

$$\delta_{red} \left(\beta = \frac{1}{2} \right) = \frac{3\sqrt{3}\, H^{\frac{1}{2}}(\nu)}{2\sqrt{2}\, \pi^2} A^2 \lambda^2 \qquad \text{(AII-5)}$$

where

$$H(\psi) = 1 + \frac{16}{9} (1-2\nu)^2 + \frac{16}{9} (1-2\nu)^4$$

The value of δ_{red} evaluated in equation (AII-5) is used in Chapter IV for deriving reduced elastic energy U_{red}.

LIST OF FIGURES

Figure

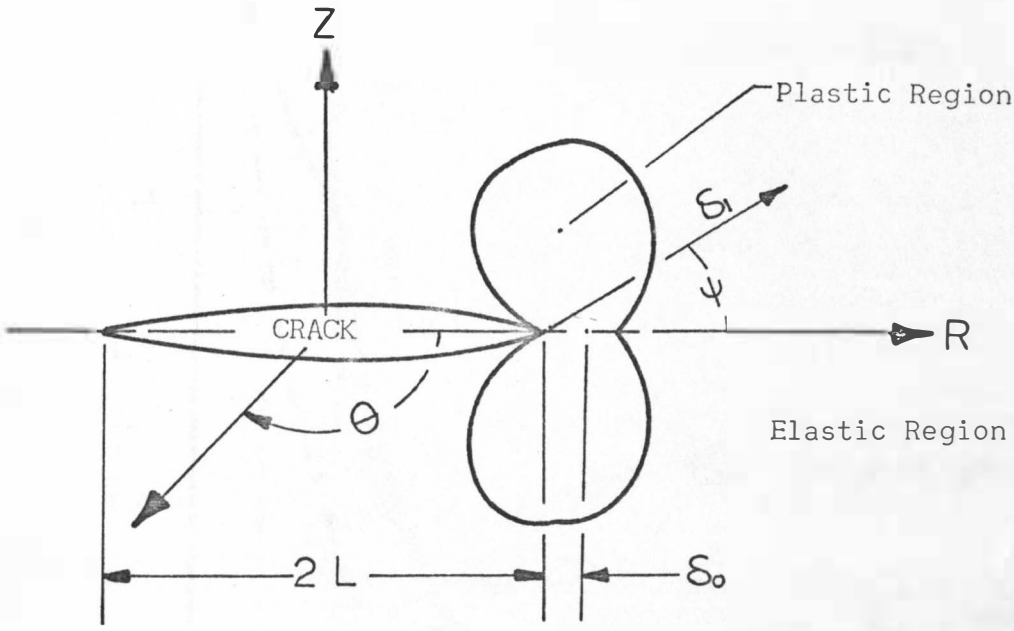

Figure 1 Geometry of Penny-Shaped Crack

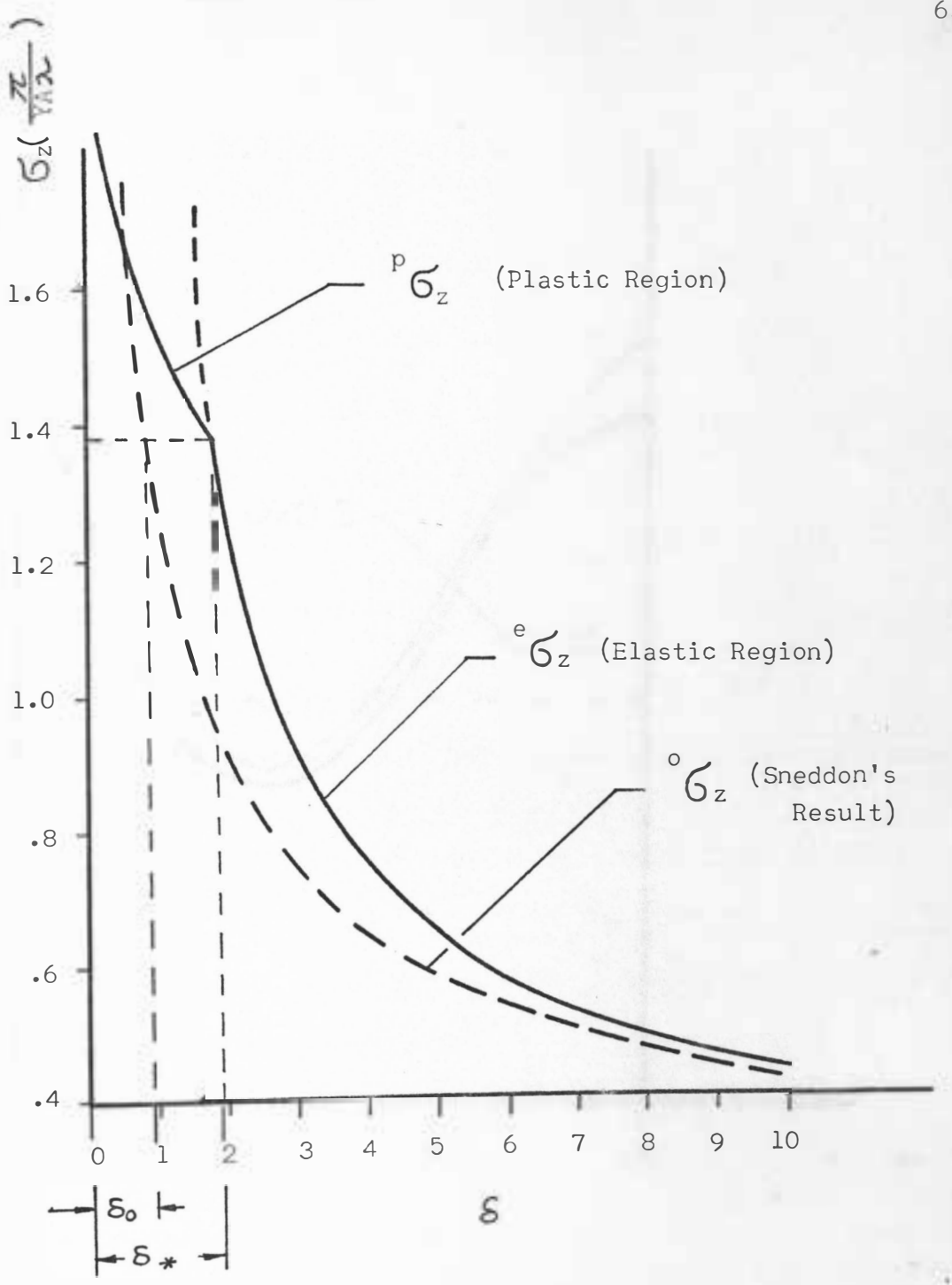

Figure 2 Comparison of Results for $\nu=0.3$, $\psi=45^o$ Strength of the Singularity $\beta=\frac{1}{2}$

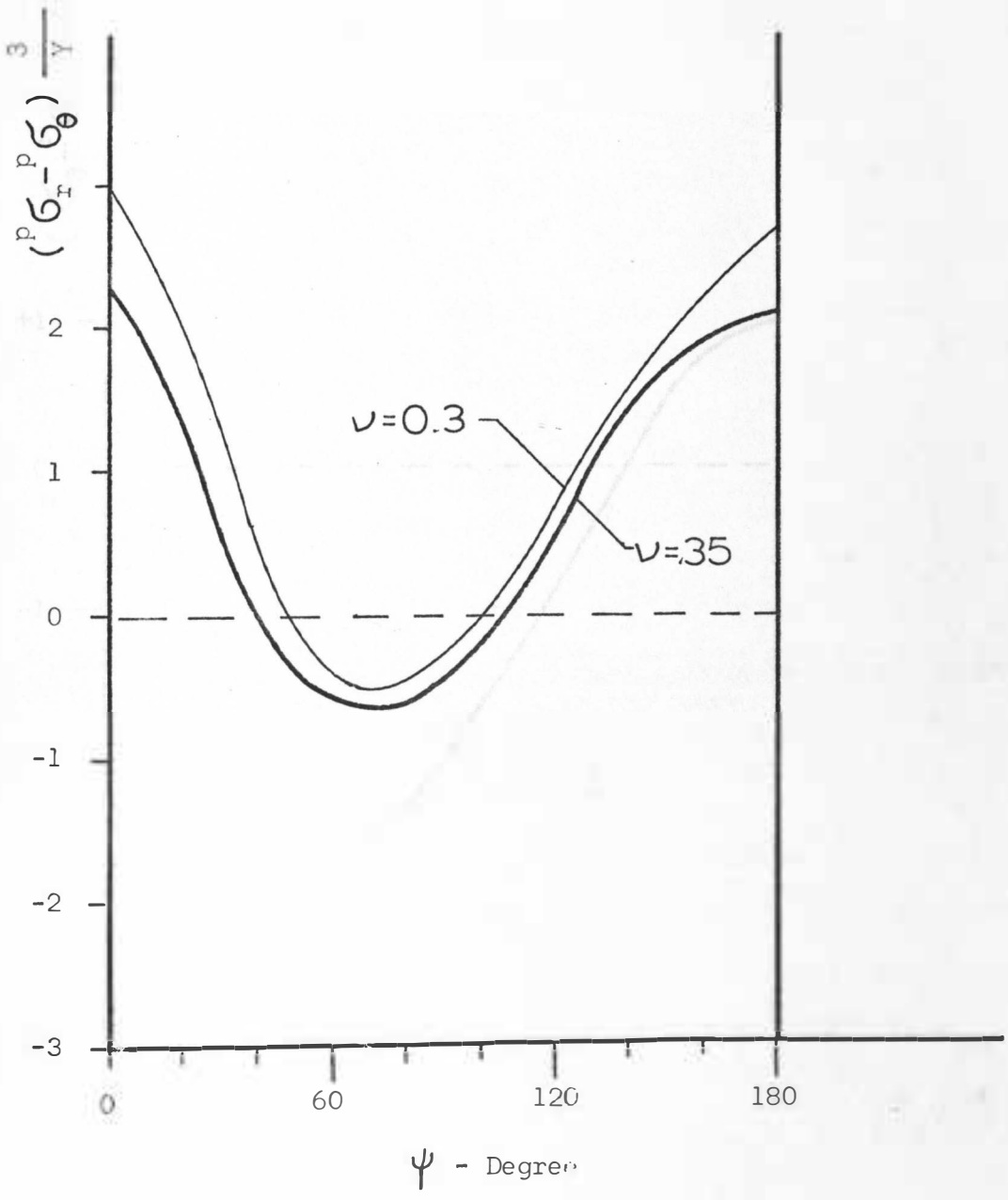

Figure 3 Distribution of First Deviatoric Stress Component

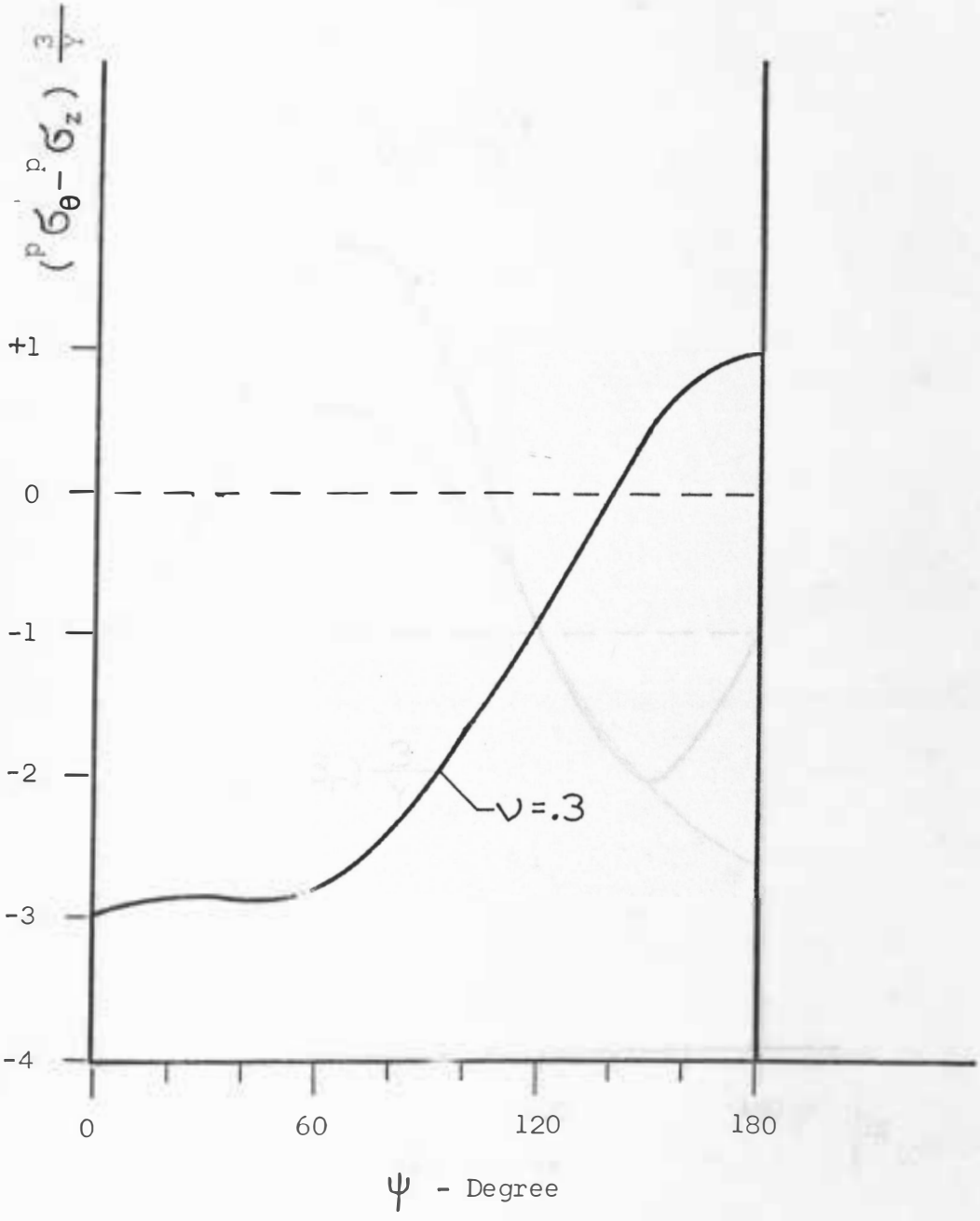

Figure 4 Distribution of Second Deviatoric Stress Component

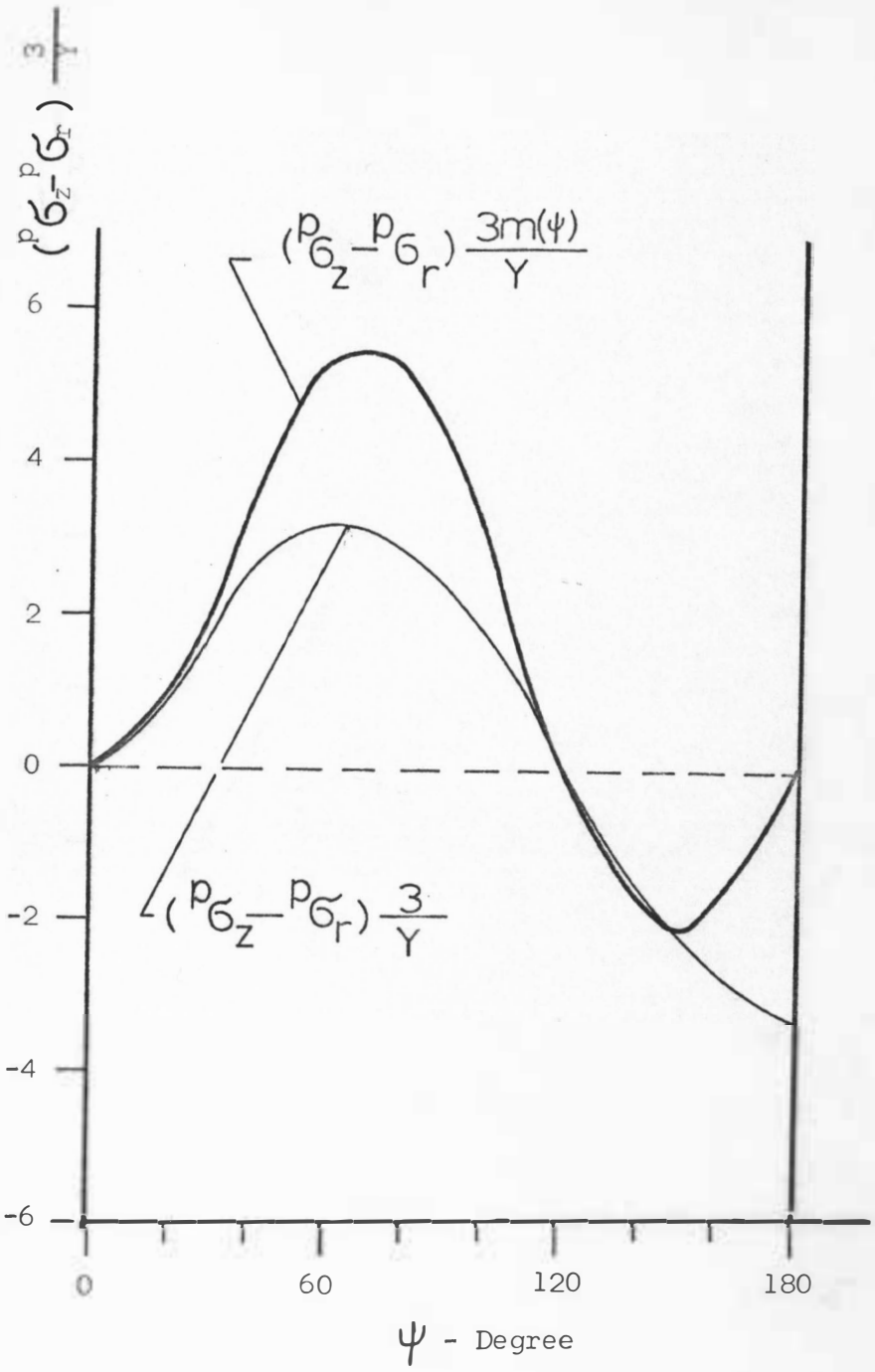

Figure 5 Distribution of Third Deviatoric Stress Component

$\upsilon = .3$

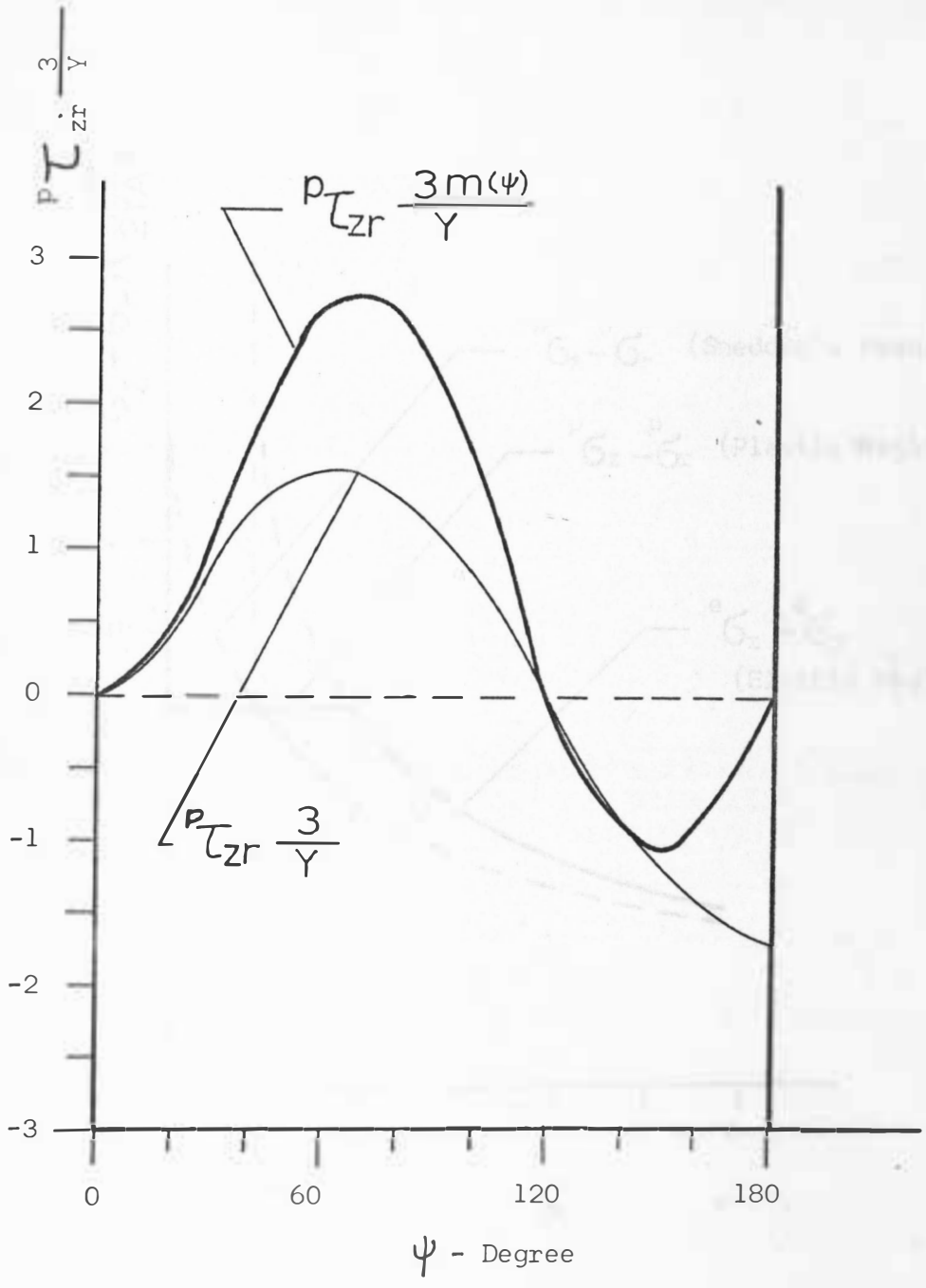

Figure 6 Distribution of Plastic Shearing Stress Component

$\nu = .3$

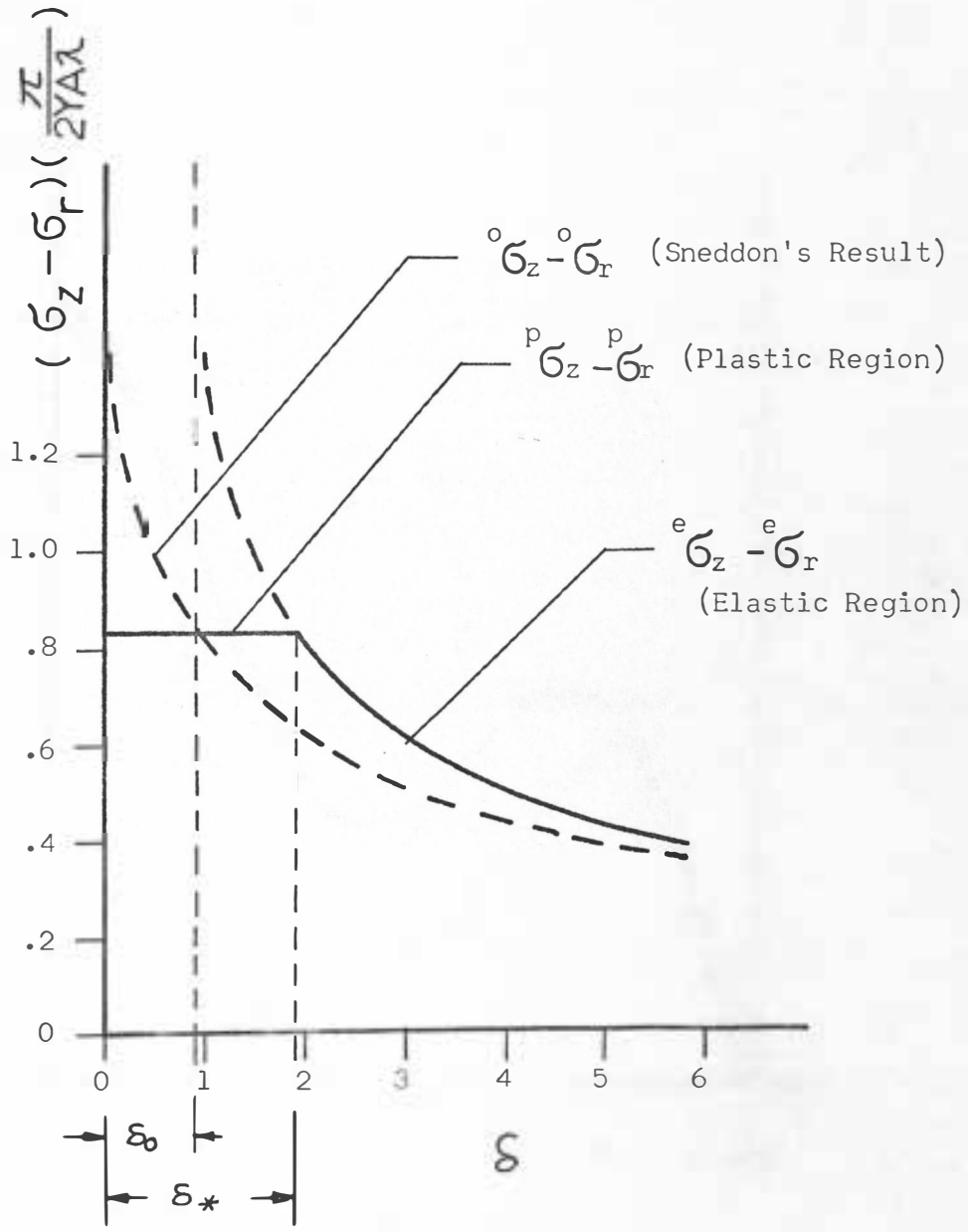

Figure 7 Comparison of Solutions for $\beta=\frac{1}{2}$, $\psi=45^{o}$

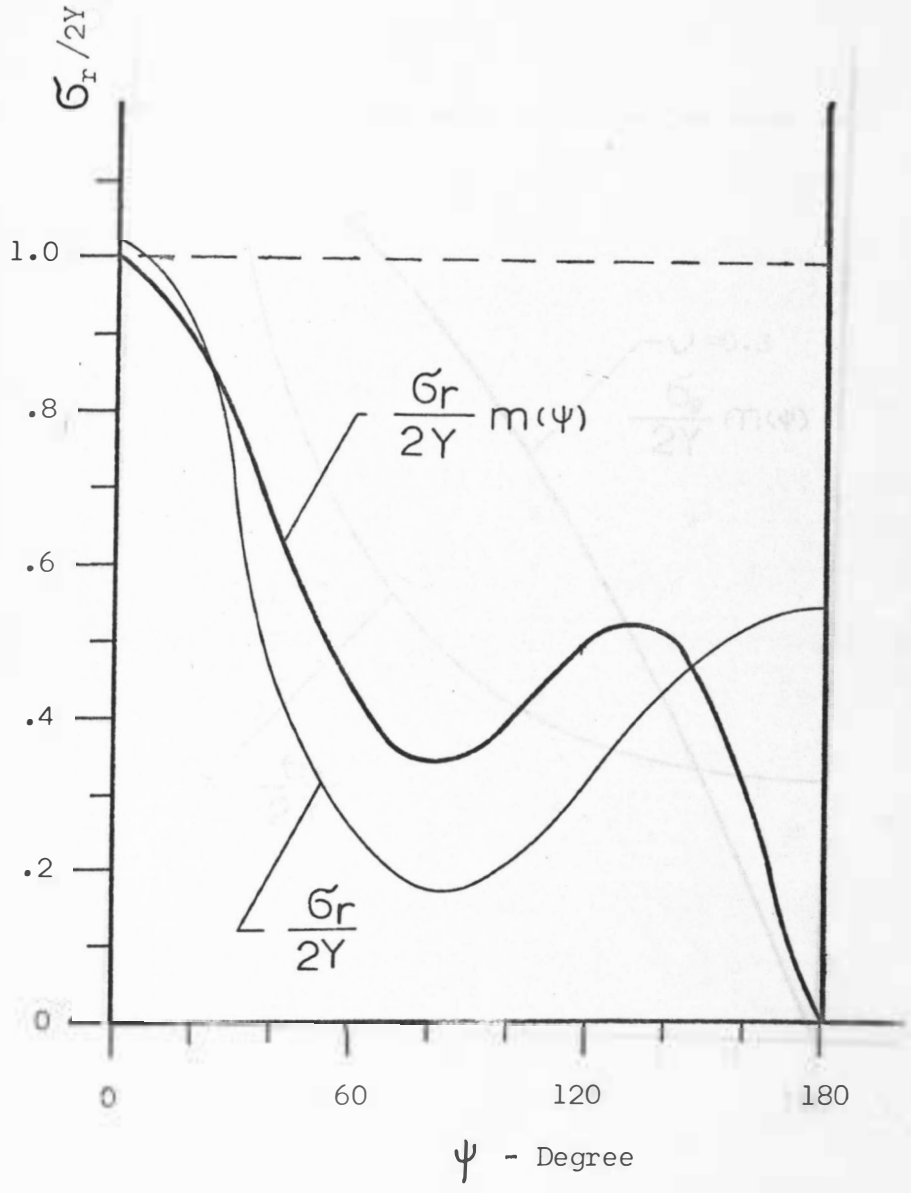

Figure 8 Distribution of σ_r Along the Elastic-Plastic Boundary

$\nu = .3$

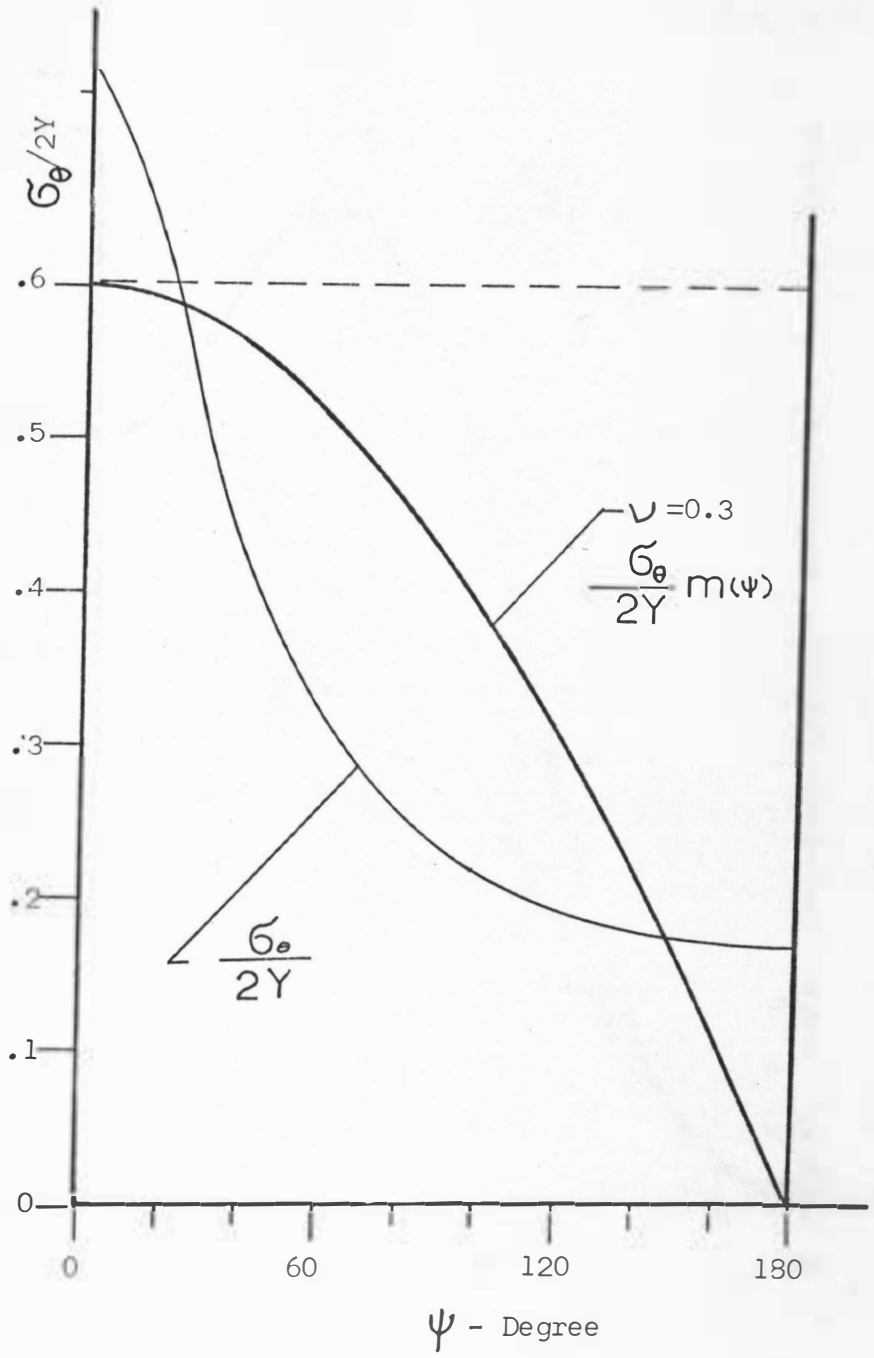

Figure 9 Distribution of σ_θ Along the Elastic-Plastic Boundary

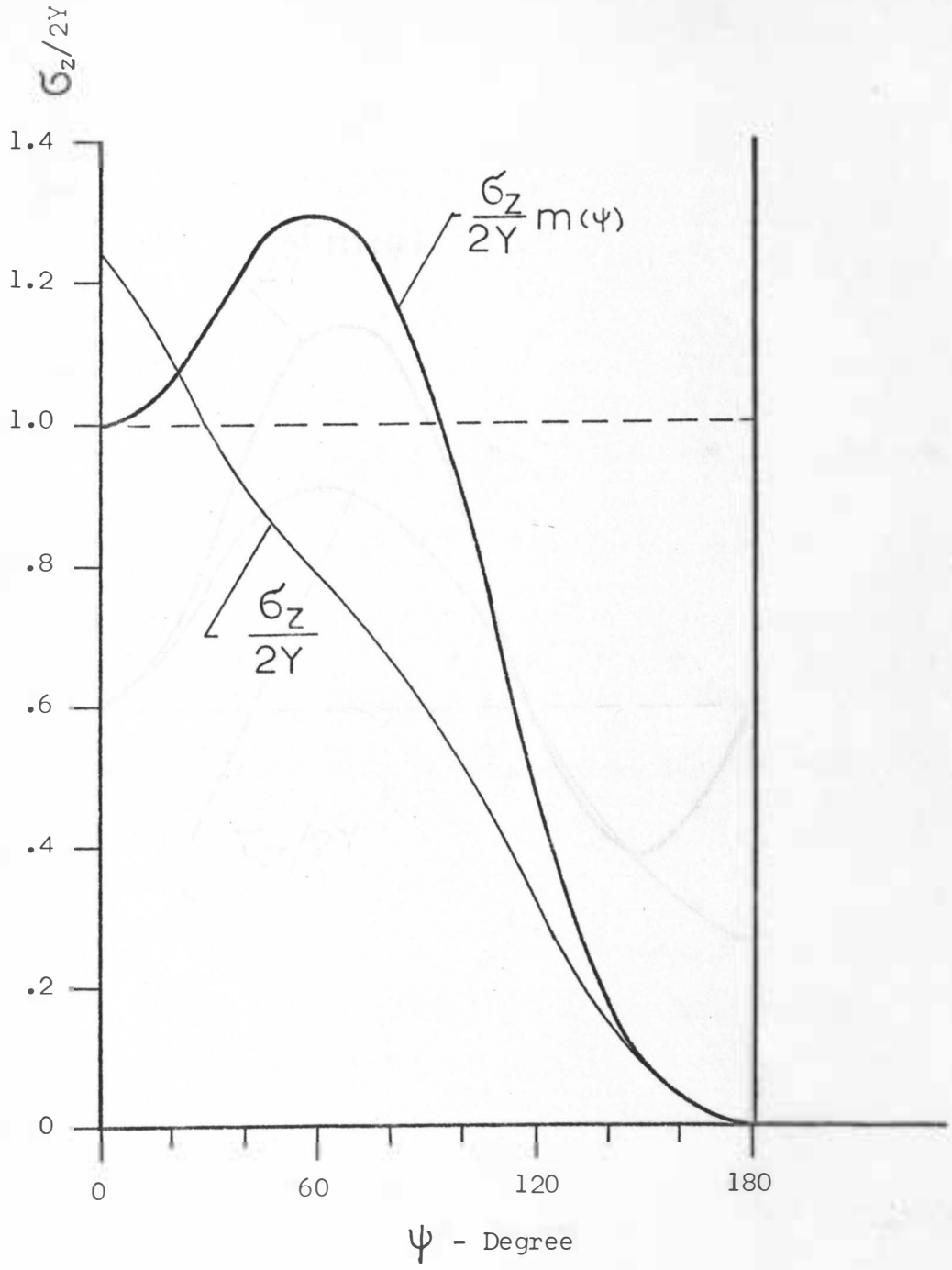

Figure 10 Distribution of σ_z Along the Elastic-Plastic Boundary

$\upsilon = .3$

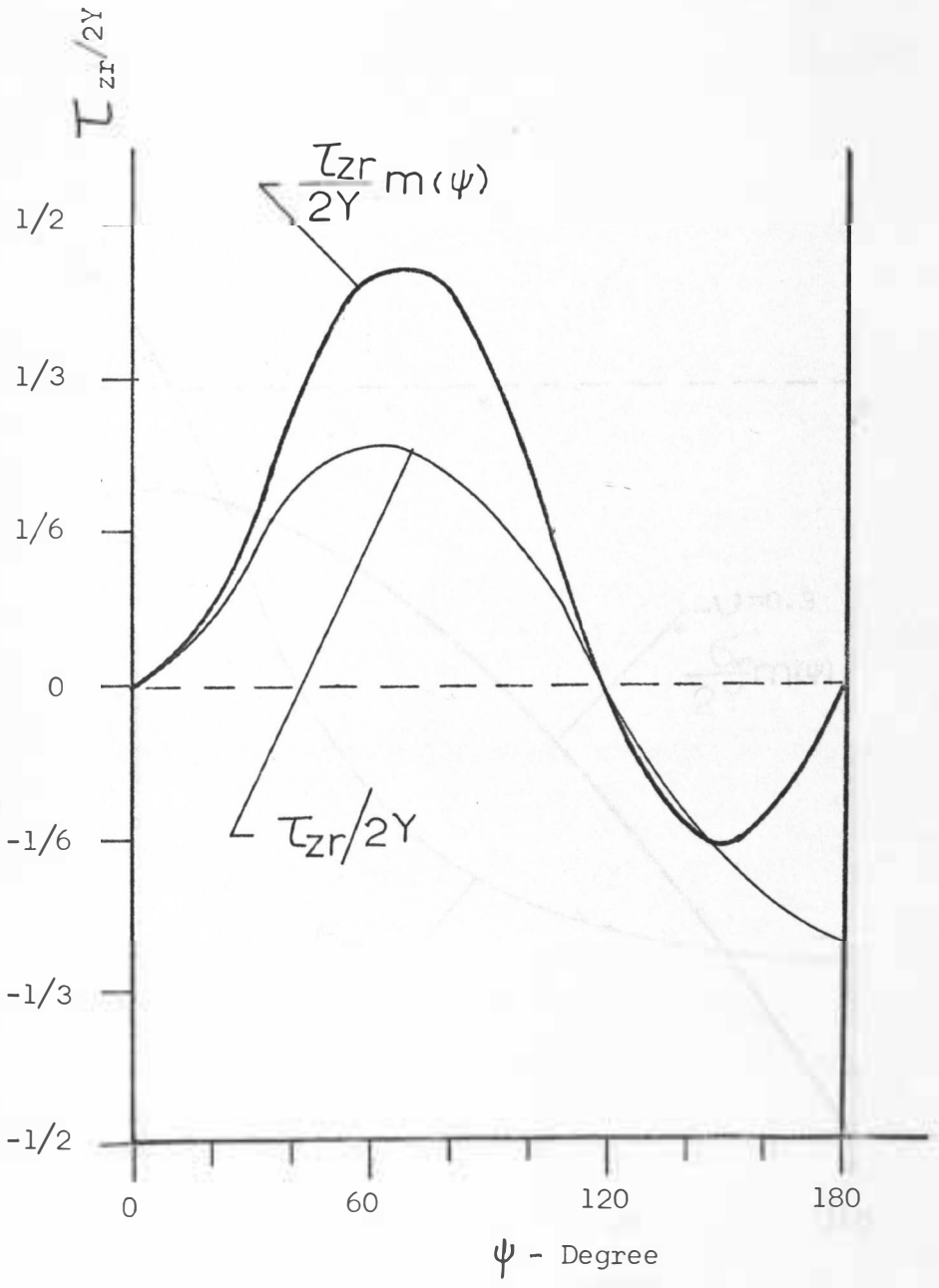

Figure 11 Distribution of τ_{zr} Along the Elastic-Plastic Boundary

$\nu = .3$

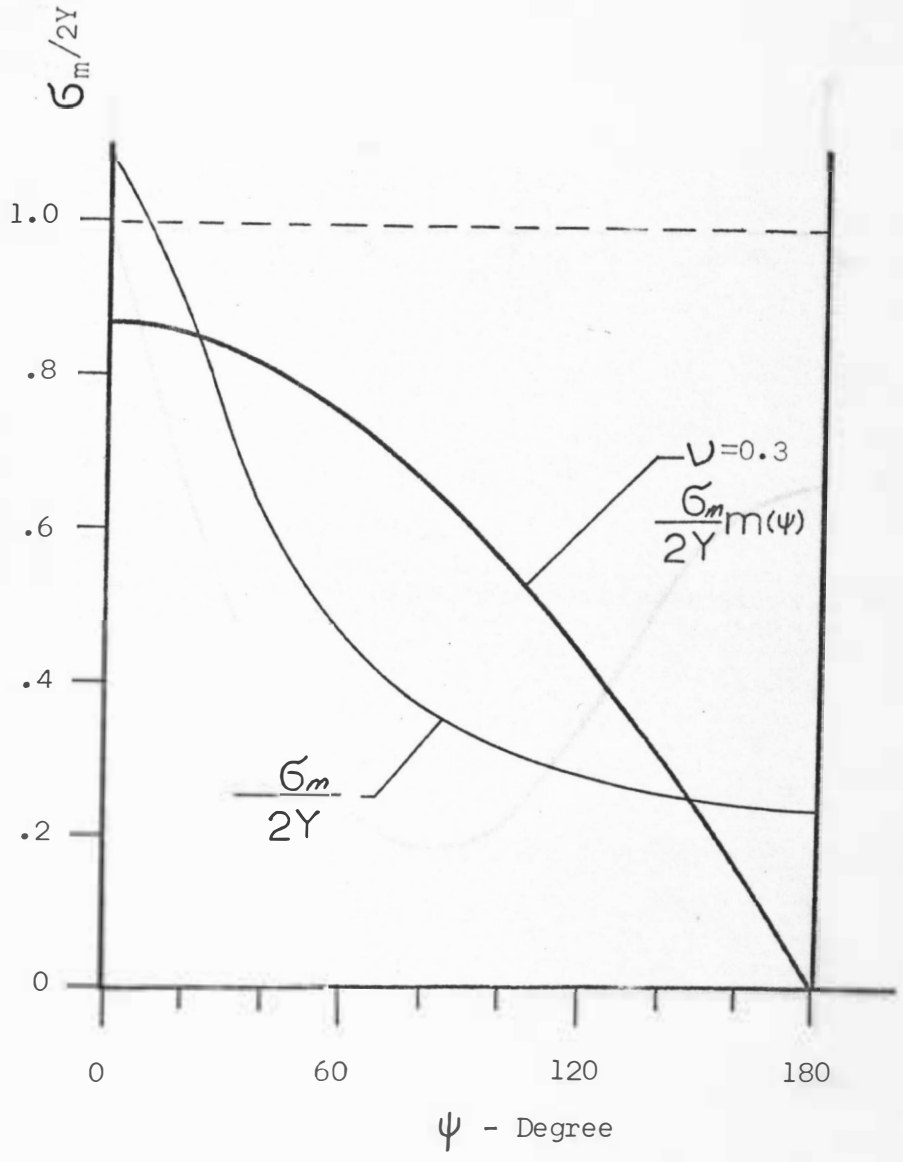

Figure 12 Distribution of σ_m Along the Elastic-Plastic Boundary

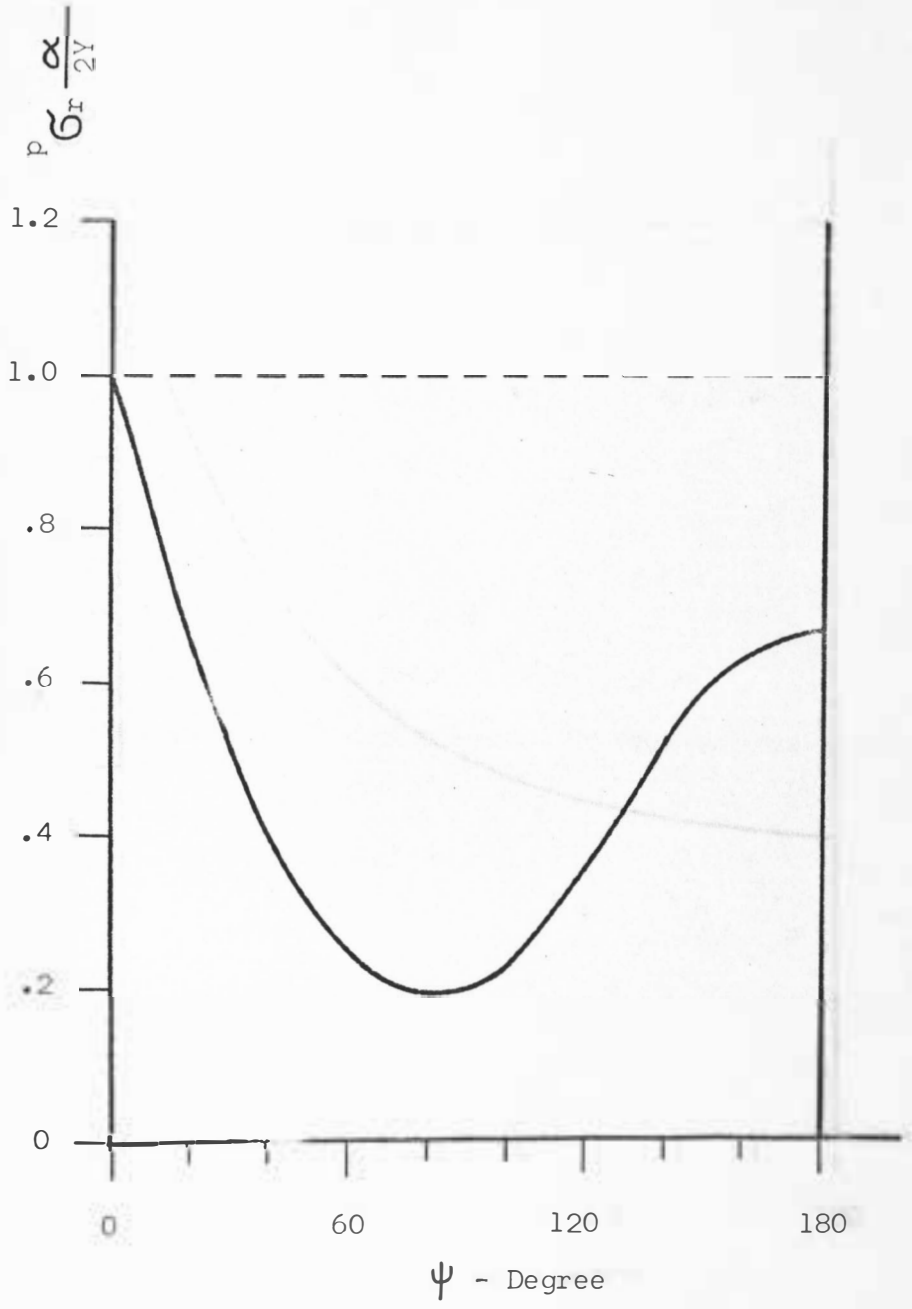

Figure 13 Distribution of $^{p}\sigma_r$ From the Maximum Principal Stress Criterion

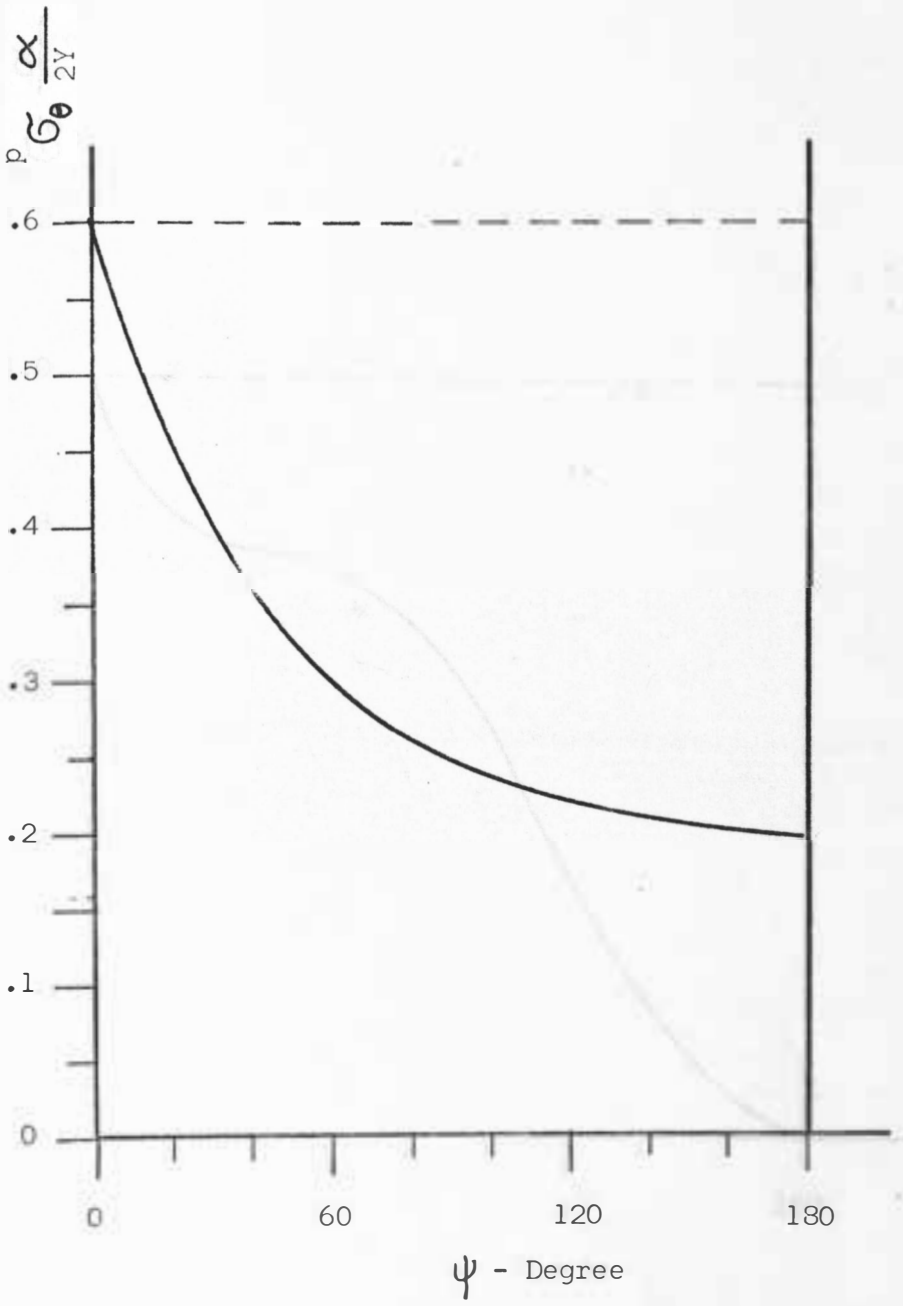

Figure 14 Distribution of ${}^{p}\sigma_\theta$ From the Maximum Principal Stress Criterion

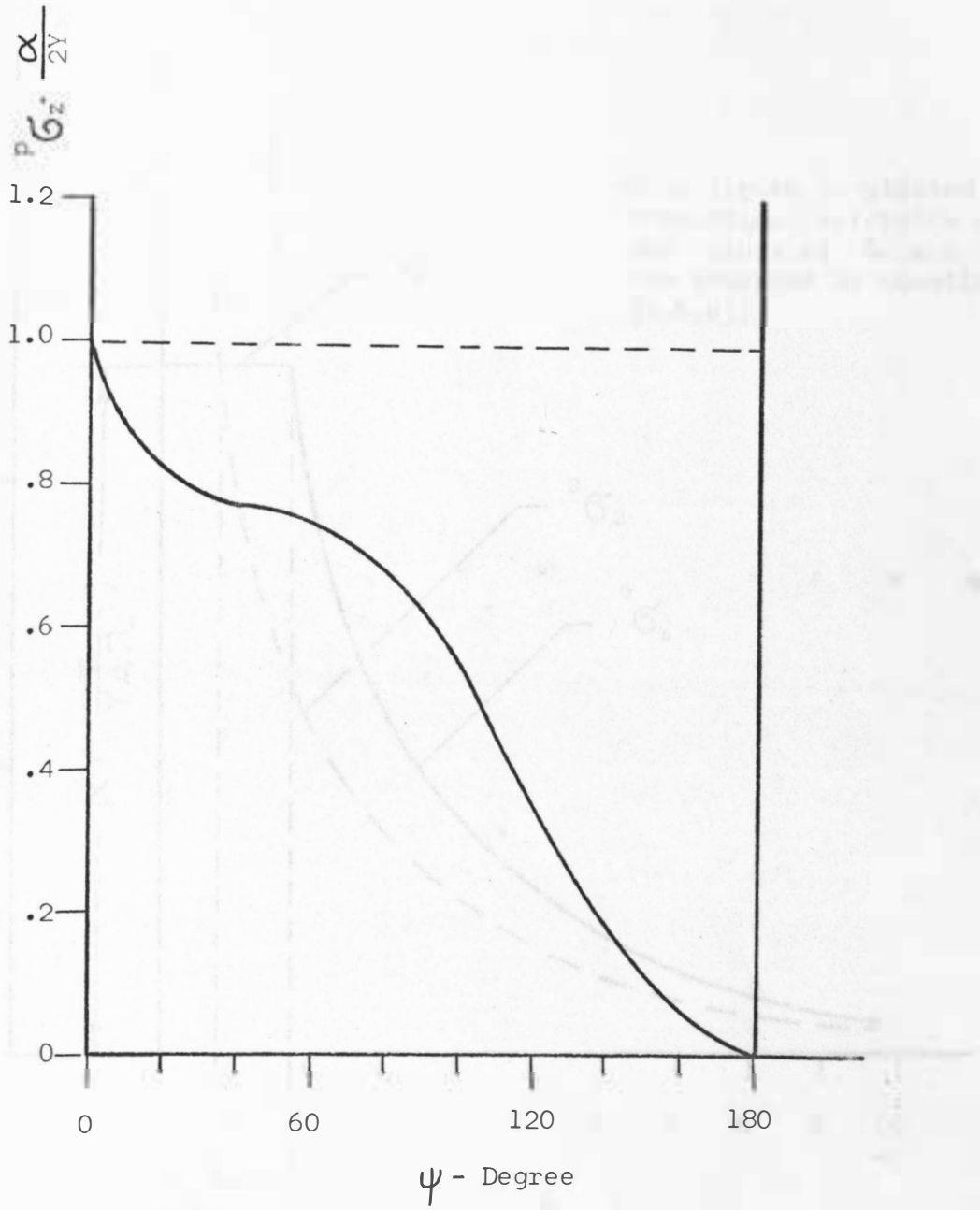

Figure 15 Distribution of ${}^{p}\sigma_z$ From the Maximum Principal Stress Criterion

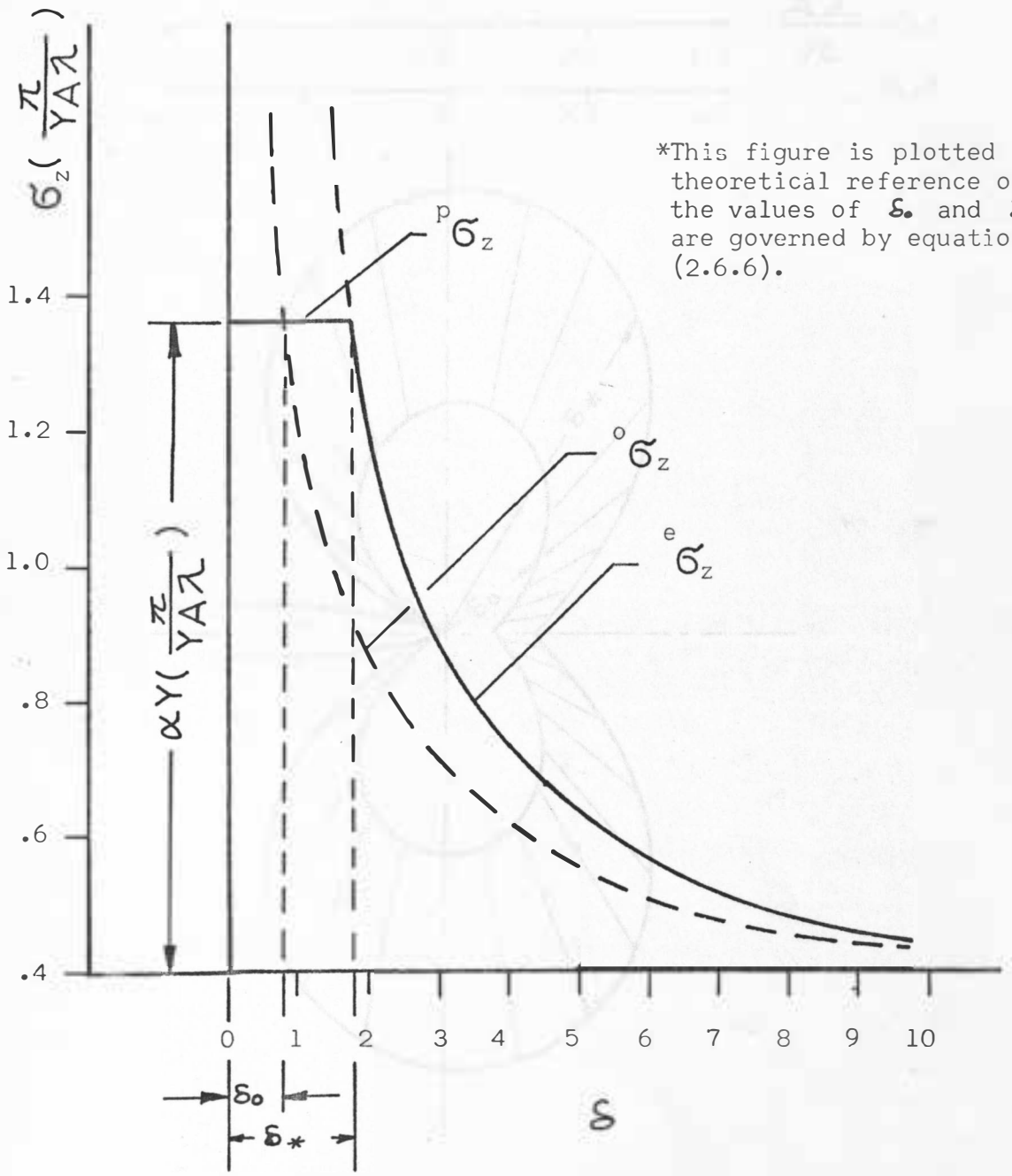

*This figure is plotted for theoretical reference only, the values of δ_o and δ_* are governed by equation (2.6.6).

Figure 16 Comparison of Stresses due to the Maximum Principal Stress Criterion for $\psi=45^o$

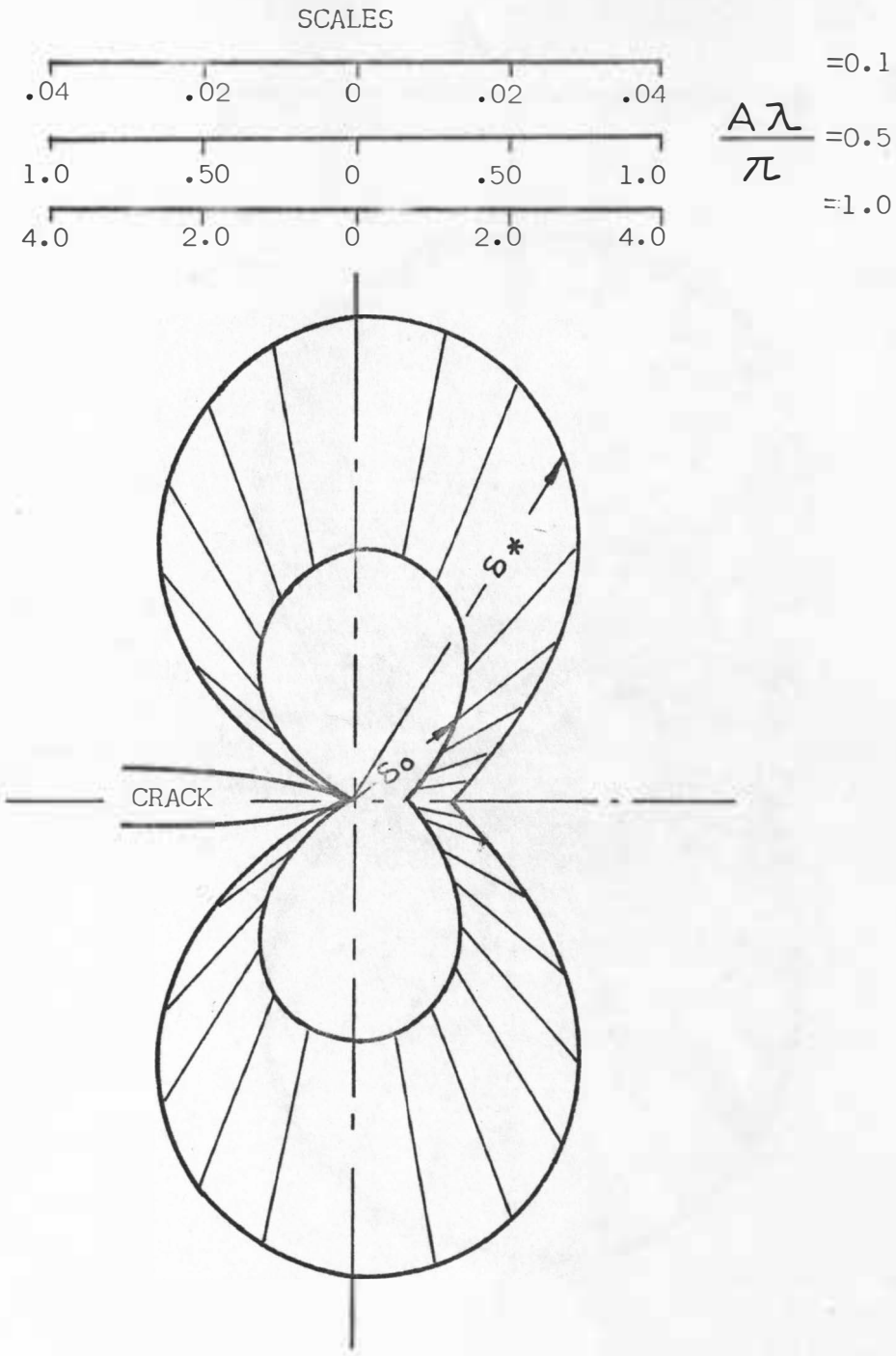

Figure 17 Contours of Elastic-Plastic Boundary & Crack Tip Shifting Distance for Brittle Materials ν =0.3

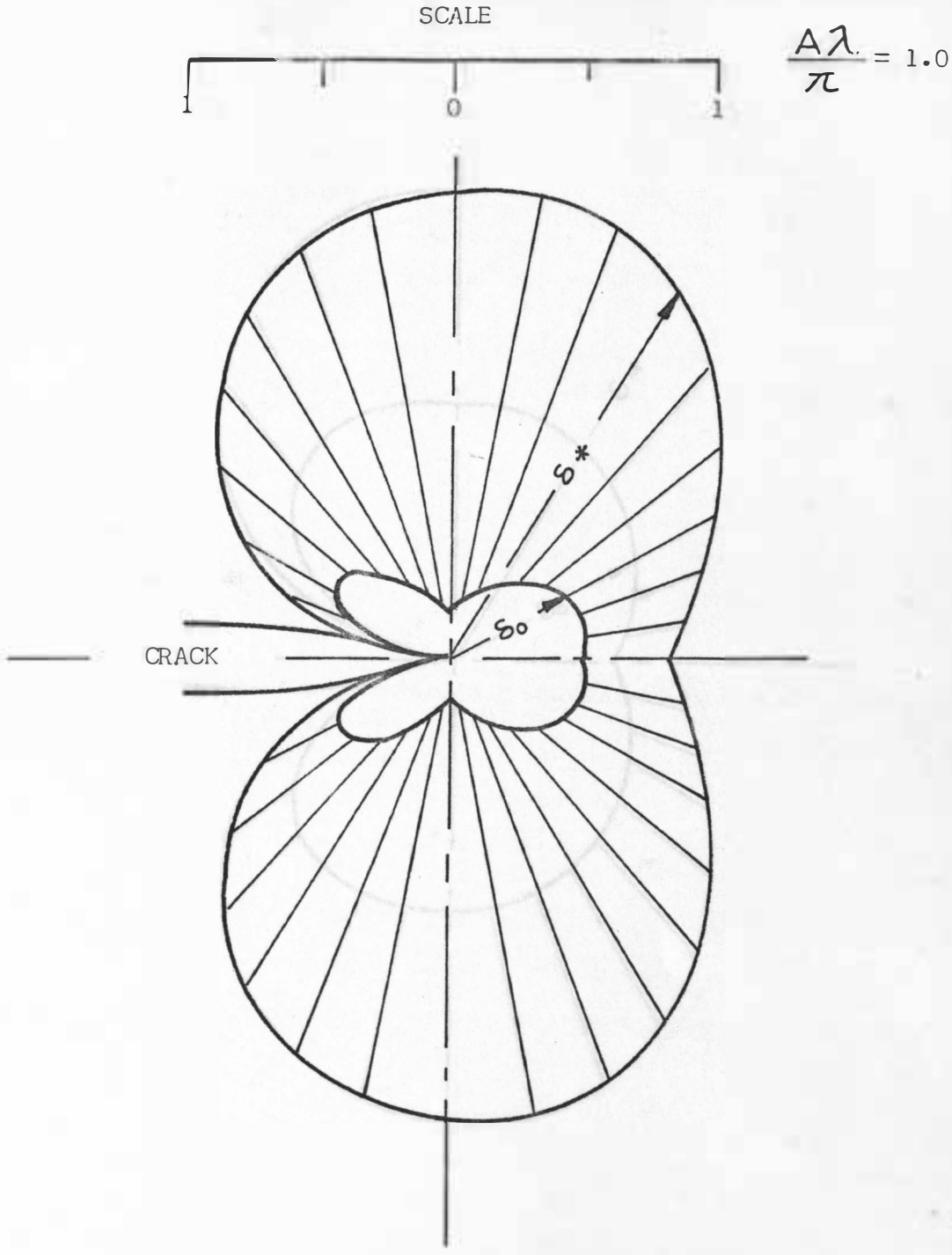

Figure 18 Contours of Elastic-Plastic Boundary & Crack Tip Shifting Distance for ν =0.3

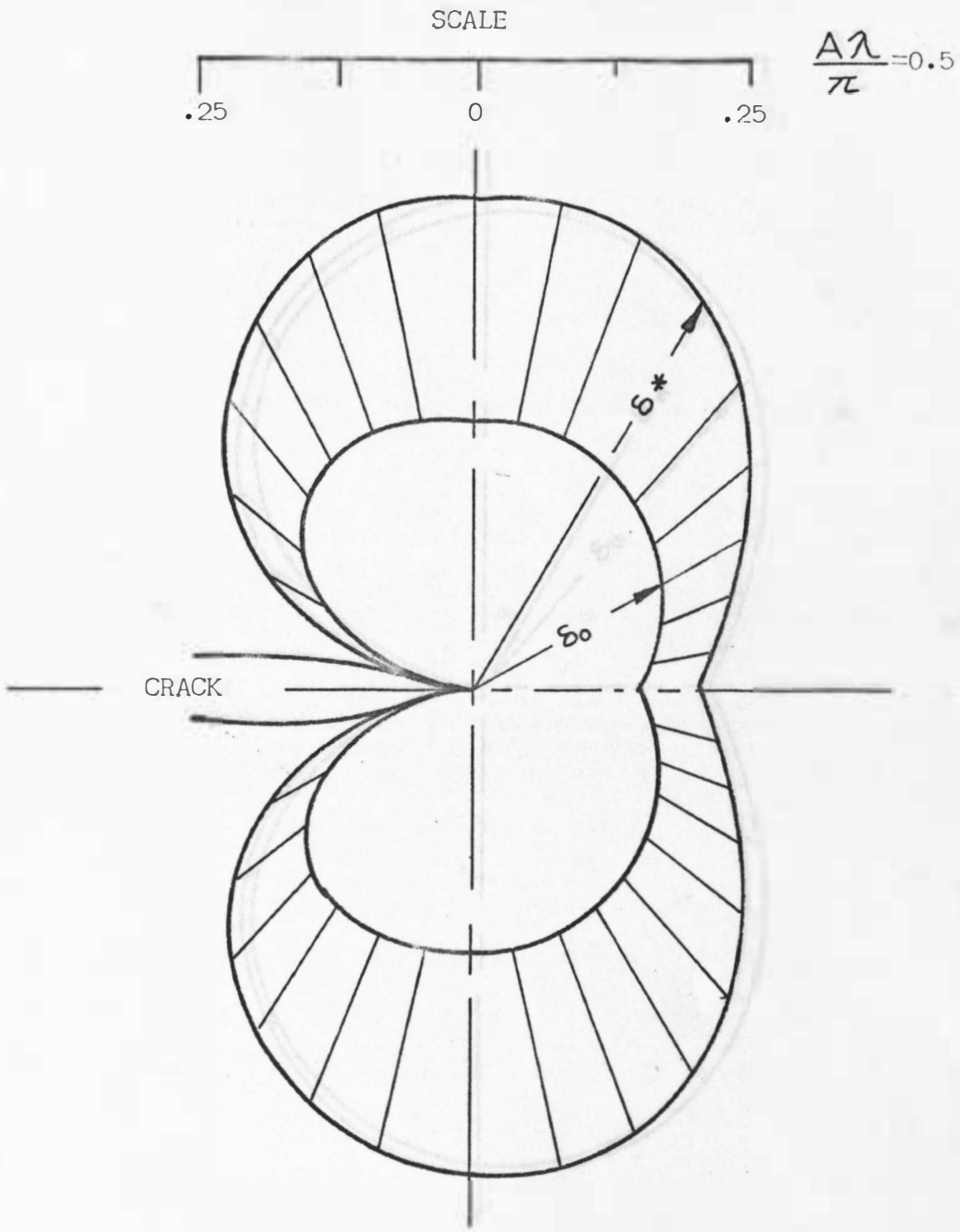

Figure 19 Contours of Elastic-Plastic Boundary & Crack Tip Shifting Distance for ν=0.3

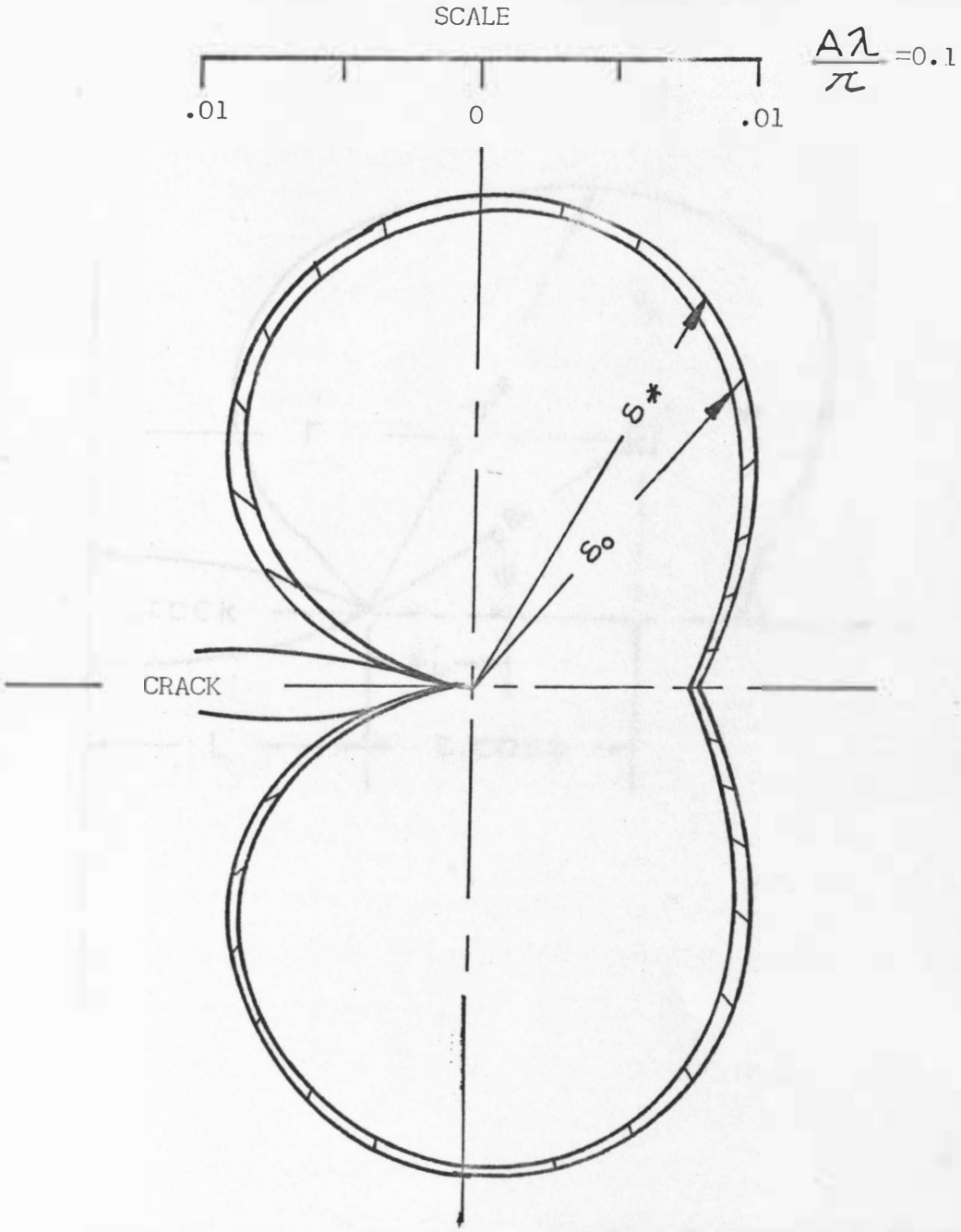

Figure 20 Contours of Elastic-Plastic Boundary & Crack Tip Shifting Distance for ν =0.3

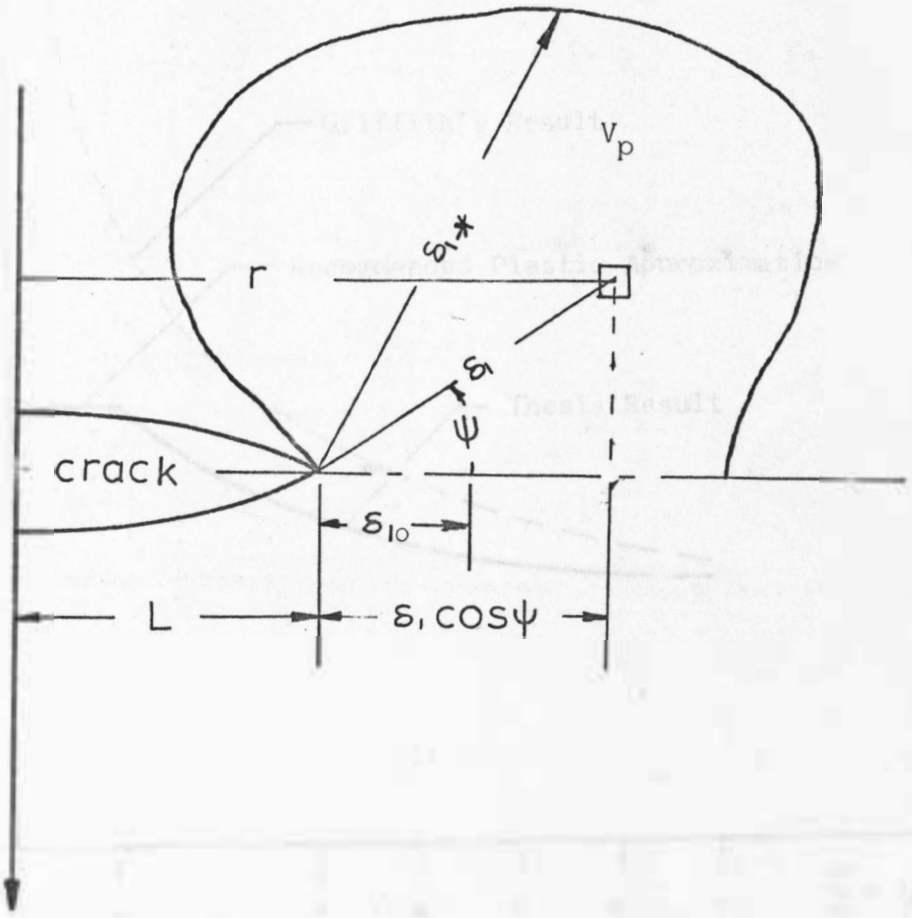

Figure 21 Coordinates for Evaluating Differential Volume

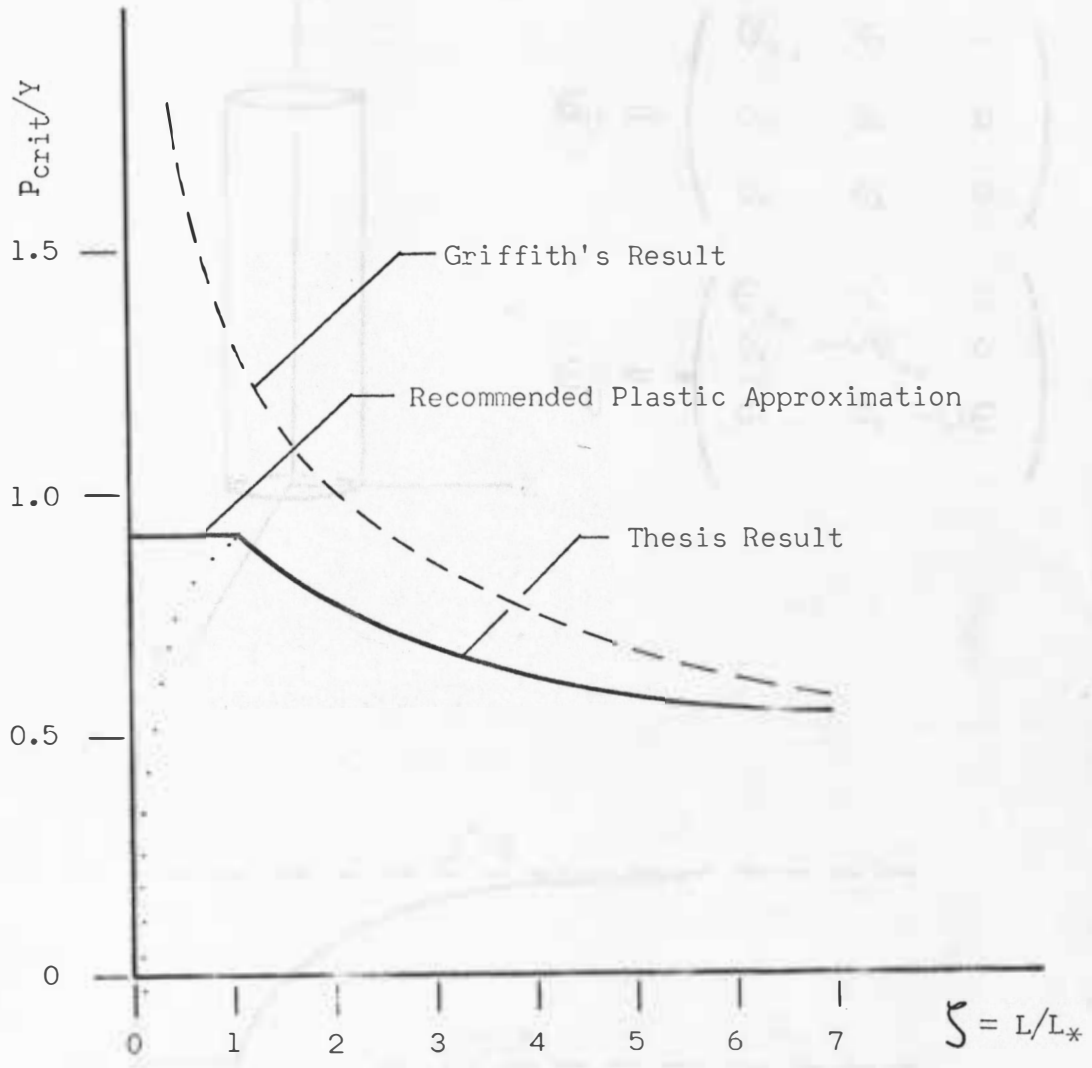

Figure 22 Comparison of Fracture Criteria

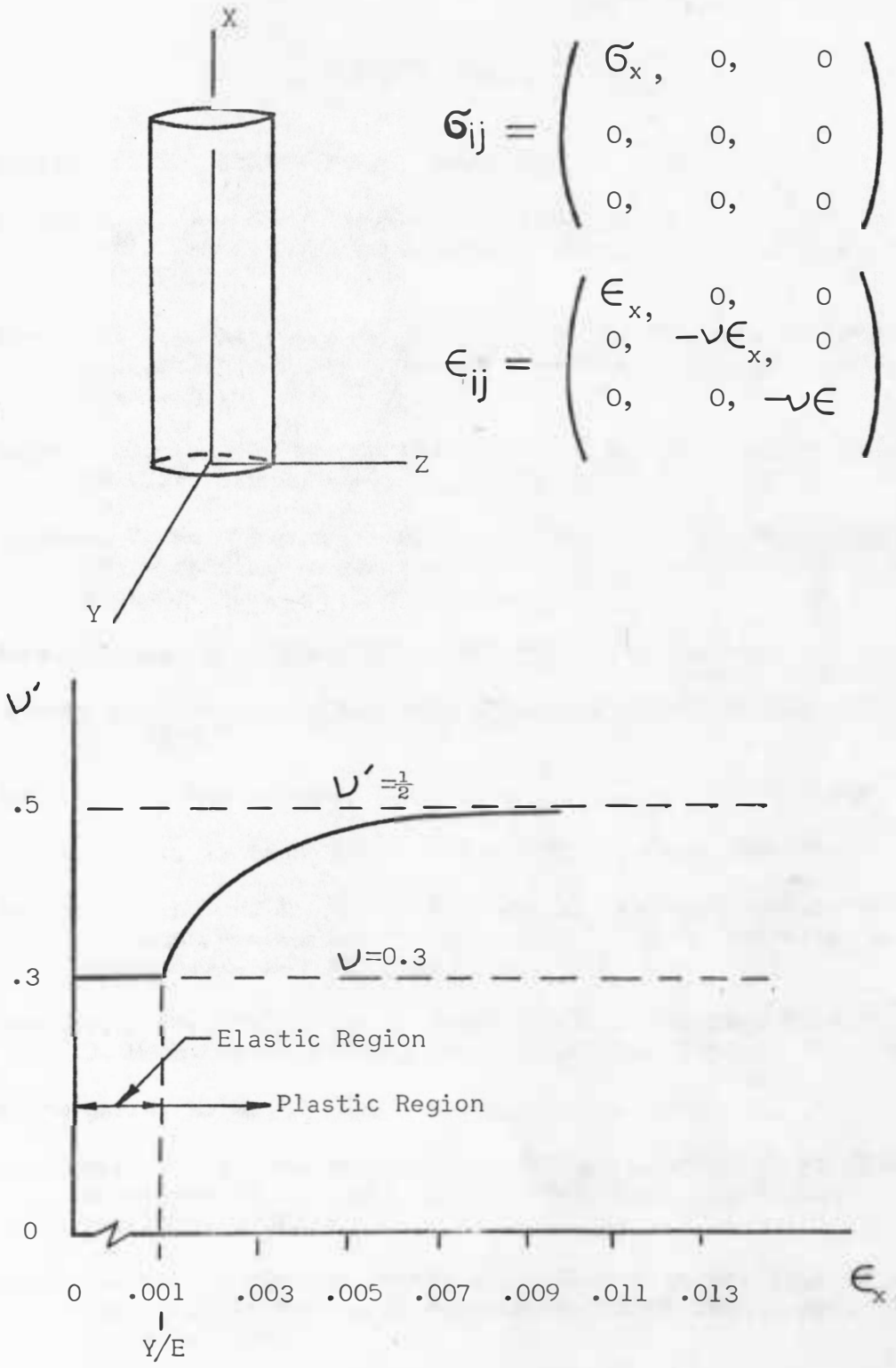

Figure 23 Coefficient of Lateral Deformation in Elastic and Plastic Regions

LITERATURE CITED

1. Inglis, C. E., Trans. Instn. Naval Archit., 1913.

2. Griffith, A. A., "The Phenomena of Rupture and Flow in Solids", Phil. Trans. Roy. Soc., London, Ser. A, Vol. 221, pp. 163-198, 1921.

3. Irwin, G. R., "Analysis of Stresses and Strains Near the End of a Crack Traversing a Plate", J. APPL. Mech., Vol. 24, Trans. ASME, Ser. E, pp. 361-364, 1957.

4. Sanders, J. L., "On the Griffith-Irwin Theory", J. Appl. Mech., Vol. 27, Trans. ASME, Ser. E, pp. 352-353, 1960.

5. Sneddon, I. N., "The Distribution of Stress in the Neighborhood of a Crack in an Elastic Solid", Proc. Roy. Soc., London, England, Vol. 187, Ser. A, pp. 229, 1946.

6. Sack, R. A., Proc. Phys. Soc., Vol. 58, pp. 729, 1946.

7. Orowan, E., "Energy Criterion of Fracture", Welding J., Vol. 34, 1955.

8. Mott, N. F., Engineering, London, Vol. 165, pp. 16-18, 1948.

9. Berry, J. P., J. Mech. Phys. Solids, Vol. 8, pp. 194-216.

10. Goodier, J. N. and Field, F. A., "Plastic Energy Dissipation in Crack Propagation", Fracture of Solids, Interscience Publishers, New York, pp. 103, 1963.

11. Dugdale, D. S., "Yielding of Steel Sheets Containing Slits", J. Mech. Phys. Solids, Vol. 8, pp. 100, 1960.

12. Westergarrd, H. M., J. Appl. Mech., Vol. 6, 1939.

13. Bueckner, H. F., "The Propagation of Crack and Energy of Elastic Deformation", J. Appl. Mech., ASME Trans., Vol. 80, pp. 1225, 1958.

14. Williams, M. L., "On the Stress Distribution at the Base of a Stationally Crack", J. Appl. Mech., ASME Trans. Vol. 79, pp. 109, 1957.

15. Wnuk, M. P., "Criteria of Ductile Fracture Initiated by a Pressurized Penny-Shaped Crack", J. Lub. Tech., Trans. ASME, pp. 56-64, Jan. 1968.

16. Wnuk, M. P., "Nature of Fracture in Relation to the Total Potential Energy", Brit. J. Appl. Phys. Ser. 2, Vol. 1, pp. 217-236, 1968.

17. Olesiak, Z. and Wnuk, M. P., "Plastic Energy Dissipation Due to a Penny-Shaped Crack", Int. J. Fracture Mechanics, Vol. 4, No. 4, Dec. 1968.

18. Mendelson, A., "Plasticity: Theory and Application", The Macmillan Co., New York, 1968.

19. Rice, J. R., "Mechanics of Crack Tip Deformation and Entension by Fatique", Fatique Crack Propagation, ASTM Special Technical Publication, No. 415, pp. 247, 1967.

20. Swedlow, J. L. and Gerberich, W. W., Proc. Soc. Exp. Stress Analysis, Series 2, Vol. 21, pp. 345-351.

21. Hutchinson, J. W., J. Mech. Phys. Solids, Vol. 13, pp. 13-31, 1965.

22. Hult, J. and McClintock, F. A., "Elastic-Plastic Stress and Strain Distributions Around Sharp Notches under Repeated Shear", Proc. of the 9th International Congress of Applied Mechanics, Brussels, Belgium, Vol. 8, pp. 51, 1956.

23. Chou, P. C. and Pagano N. J., "Elasticity-Tensor, Dyadic, and Engineering Approaches", D. Van Nostrand Co., Inc.

24. Sadeghi, M., "Penny-Shaped Crack in an Elastic-Plastic Solid", Master's Thesis, S. D. S. U., 1969.

25. Bridgman, P. W., "Studies in Large Plastic Flow and Fracture", Harvard University Press, Cambridge, Massachusetts, 1964.